Title: Structure of the paraplacenta and the yolk sac placenta of the viviparous Australian sharpnose shark, *Rhizoprionodon taylori*

Authors: Alice L. Buddle[1], James U. Van Dyke[2], Michael B. Thompson[1], Colin A. Simpfendorfer[3], Christopher R. Murphy[4], Samson N. Dowland[4] and Camilla M. Whittington[1,]

[1] School of Life and Environmental Sciences, The University of Sydney, Heydon-Laurence Building (A08), Sydney, NSW 2006, Australia.

[2] Department of Pharmacy and Biomedical Science, School of Molecular Sciences, La Trobe University, Wodonga, Victoria, Australia

[3] College of Science of Engineering, James Cook University, Townsville, Queensland, Australia

[4] School of Medical Sciences (Anatomy and Histology), The University of Sydney, Sydney, New South Wales, Australia

Correspondence: Camilla M. Whittington

Email address: camilla.whittington@sydney.edu.au

Postal address: Camilla M. Whittington, School of Life and Environmental Sciences, Heydon-Laurence Building (A08), Sydney, NSW 2006, Australia

Funding: Australian Research Council, Grant/Award Number: DP1801103370

© 2021. This manuscript version is made available under the CC-BY-NC-ND 4.0 license
https://creativecommons.org/licenses/by-nc-nd/4.0/

Abstract

Introduction

Viviparity (live-birth) has evolved from oviparity (egg-laying) multiple times in sharks. While most transitions from oviparity to viviparity have resulted in non-placental forms of viviparity, some sharks develop a yolk sac placenta during pregnancy. The Australian sharpnose shark (*Rhizoprionodon taylori)* is a placental species that suspends embryonic development in a diapause for most of pregnancy.

Methods

To identify structures involved in supporting rapid embryonic growth in late pregnancy, we examined uterine and placental morphology by light and electron microscopy.

Results

Paraplacental uterine regions have morphological specialisations consistent with secretion and fluid transport between uterine tissues and the lumen. Uterine secretions in the lumen may be absorbed by the outgrowths on the embryonic umbilical cord ('appendiculae'), which are densely covered by microvilli. The placenta consists of uterine villi that interdigitate with the yolk sac and enhance the surface area available for fetomaternal exchange. The yolk sac does not invade the uterine epithelium, and the egg capsule remains intact at the placental interface, separating maternal and fetal tissues. Some placental uterine epithelial cells are secretory, and endocytic vesicles in the opposing yolk sac ectodermal cells suggest that nutrient transport is by histotrophic uterine secretion followed by fetal absorption. Respiratory gases, water and possibly small nutrients likely diffuse across the placenta, where maternal and fetal blood vessels are ~ 2 µm apart.

Discussion

Placental structure in *R. taylori* is similar to most other sharks, but there are differences in cellular structures between species that may indicate species-specific placental transport mechanisms.

Keywords: pregnancy; uterus; chondrichthyans; electron microscopy

- Placentae of *Rhizoprionodon taylori* consist of uterine villi and fetal yolk sac
- The uterine villi are separated from the fetal yolk sac tissue by an egg capsule
- Placental morphology indicates a gas exchange and nutrient transfer function
- Paraplacental uterine morphology is consistent with secretion and fluid transport

Manuscript + References
Click here to access/download;Manuscript + References;placenta paper final.doc

Introduction

Viviparity (live-birth) has evolved independently from oviparity (egg-laying) over 150 times in vertebrates [1]. The evolution of viviparity in amniotes (mammals and reptiles) involves the development of placentae for physiological exchange between fetal and maternal tissues during pregnancy [2,3]. In contrast, while most sharks are viviparous, placentae are only present in species from five shark families (Carcharhinidae, Sphyrnidae, Hemigaleidae, Leptochariidae and Triakidae) within the order Carcharhiniformes (ground sharks; [4]).

The placenta may develop in viviparous sharks to provide embryos with a substantial amount of nutrients during pregnancy (placentotrophy; [5]; [6]). In addition to placentotrophy, viviparous sharks have a diverse range of non-placental ways to nourish embryos during pregnancy: lecithotrophy ("yolk-feeding"; embryos rely on nutrients contained in the egg yolk); histotrophy (embryonic absorption of maternal secretions); histophagy (embryonic ingestion of nutritive secretions); oophagy (embryonic ingestion of unfertilised eggs) and adelphophagy (embryonic ingestion of siblings; [7,8]). Placental formation involves ontogenetic and physiological transformations of fetal and maternal tissues during pregnancy and is therefore morphologically more complex than non-placental forms of viviparity [8,9]. The multiple non-placental ways in which sharks support embryonic nourishment make the evolutionary advantage of placental viviparity unclear [8].

Non-placental mechanisms are used to nourish all placental sharks during pregnancy [1,8]. For example, embryos are initially lecithotrophic, with the placenta forming after the yolk nutrients have been consumed [5]. In addition to the yolk nutrients, histotrophic uterine secretions may provide embryos with nutrients before and after placental development [7]. These secretions may be ingested through the mouth of developing embryos, or absorbed by the fetal gill epithelium and/or the accessory placental structures (appendiculae) on the umbilical cord of some species (e.g. *R. terraevonvae;* [10] and *Sphryna tiburo;* [11]). In most species, the placenta forms 2- 4 months into pregnancy [4]. Shark placentae range from the simple apposition of the yolk sac to a vascularised uterine wall (e.g. *Prionace glauca;* [12]) to complex placental interdigitations between the yolk sac and uterine tissues (e.g. *Rhizoprionodon terraenovae* and *Carcharhinus plumbeus;* [10,13]). In all species investigated

so far, the yolk sac does not invade through the uterine mucosa during placental formation and the embryonic egg capsule usually separates the yolk sac from the uterine mucosa [7]. Nutrient transport across the shark placenta is likely by uterine histotrophic secretion followed by fetal absorption, rather than hemotrophic transfer (nutrient transfer directly between fetal and maternal blood streams; [7]). However, firm conclusions about placental function and evolution in sharks require morphological data from a wider range of species [8].

Here, we combined light and electron microscopy to provide the first detailed morphological description of uterine and placental tissues in the Australian sharpnose shark, *Rhizoprionodon taylori* (Carcharhinidae; [14]). *Rhizoprionodon taylori* has an embryonic diapause period: embryos are suspended in a diapause from the blastodisc stage for seven months of the 11.5-month gestation (Fig. 1; [14,15]). A placenta does not exist during the diapause period, so it serves as a 'pre-placental' state for *R. taylori*. We compare the morphologies of the uterus in both the embryonic diapause period and the placental period to identify structures that develop late in pregnancy to support embryonic growth and development in the final 3 to 4 months of gestation. In the placental period, we identify tissues that are likely to be important for physiological exchange during pregnancy in sharks: the umbilical cord appendiculae, the paraplacental uterus and the fetomaternal placental interface [7]. Since embryonic growth increases exponentially after the placenta forms in *R. taylori* (Fig. 1), we predicted that the uterine and yolk sac tissues would be specialised for respiratory gas exchange, waste removal and nutrient transport. Like other placental sharks, we predicted that placental morphology in *R. taylori* reflects histotrophic, rather than hemotrophic, placental nutrient transport [7].

Methods

Field collection

Female *R. taylori* were collected by mesh monofilament gillnets in Cleveland Bay, north Queensland. Early pregnant (n=6) females were collected in June and late pregnant females (n=10) were collected in December. Non-pregnant, sexually mature females are rarely caught because mating occurs almost immediately after parturition in *R. taylori* [14]. Therefore, we did not collect non-pregnant females for this study. Immediately after capture, females were euthanised by severing the spinal cord with a sharp knife. Embryos in the diapause stage (blastodisc, [16]) were present in the early pregnant uteri. In late pregnant females, large embryos, almost completely developed and pigmented, were attached to the uterine wall by an umbilical cord and placenta [16]. All research activities were conducted under the permit requirements of the Great Barrier Reef Marine Park Authority - GBRMPA (G15/37987.1) and the Queensland Department of Primary Industries and Fisheries – DPI (187250 and 200906). The protocol was approved by the James Cook University Animal Ethics Committee (permit no. A2310) and the University of Sydney Animal Ethics Committee (permit no. 2019/1583).

Light microscopy

Small (1 cm^3) pieces of uterine tissue were dissected out of the paired uteri of early pregnant females (n=6). Pieces of uterine, placental and umbilical cord tissues were dissected out of late pregnant females (n=10). All tissues were immediately fixed in 10 % NBF (neutral buffered formalin) for 4 - 6 h. The tissues were then dehydrated to 100 % ethanol and infiltrated with paraffin wax. Paraffin embedded tissue samples were sectioned at 7 µm thick on a Tissue-Tek Accu-Cut™ microtome (Sakura, Tokyo, Japan) and mounted onto glass slides. Slides were dried at 37 °C for 12 h. To examine the structure of the tissues, sections were cleared with histolene, rehydrated through a series of ethanol concentrations, rinsed with water and then stained with Harris hematoxylin and Putt's eosin. The combined Alcian blue (AB)/periodic acid-Schiff (PAS) procedure (pH of Alcian blue = 2.5) was used to detect PAS-positive material (e.g, neutral mucosubstances, carbohydrate moieties and portions of the basement membrane) and Alcian blue positive- acidic

mucosubstances [17]. Glass coverslips were placed over the sections using BDH DPX mounting medium (Fronine Laboratory Supplies, NSW, Australia). A Zeiss deconvolution microscope (Carl Zeiss Pty. Ltd., Australasia) in brightfield mode was used to view the slides and images were taken using a Zeiss AxioCam HR digital colour CCD camera (Carl Zeiss Pty. Ltd., Australasia). All images were labelled and processed using Adobe photoshop 2021 (22.1.1).

Enzyme histochemistry

Uterine and placental tissues collected from late pregnant females for enzyme histochemistry (n=5) were stored in Tissue-Tek OCT cryoprotectant (Sakura, Tokyo, Japan) in liquid nitrogen. A Leica CM3050 S cryostat (Leica, Heerbrugg, Switzerland) was used to cut sections of uterine and placental tissues at 7 µm thickness. Twelve sections of uterine and placental tissue were collected for each female on gelatin-coated slides. Two experimental slides and two control slides were collected per female. Experimental slides were stained for the presence of either alkaline or acid phosphatase enzyme using a modified Gomori technique [17,18]. Alkaline phosphatase enzyme is associated with active transport in secretory cells and therefore may be involved in histotrophic placental nutrient transport [19]. Experimental slides for alkaline phosphatase staining were incubated for 1 h in a filtered solution of 3% sodium β-glycerophosphate, 0.25 % lead nitrate and 0.05M barbital buffer (pH 9.0; [17,18]. Acid phosphatase enzyme indicates the presence of lysosomes, which may also be involved in histotrophic nutrient transport by breaking down macromolecules into smaller components for uterine secretion [17,19,20]. Experimental slides for acid phosphatase staining were incubated for 30 min in a filtered solution of 0.4 % sodium β-glycerophosphate, 0.5 % lead nitrate and 0.2 M acetate-acetic acid buffer (pH 4.7; [17]). Sodium β-glycerophosphate was omitted from the incubation medium for the negative control slides [17]. All slides were incubated at 28 °C, the mean body temperature of *R. taylori* in December [16]. After incubation, slides were immersed in 0.5% ammonium sulphide solution for 30 s. The slides were then rinsed in three changes of water and mounted with Hydromount (Geneworks). Slides were viewed with a Zeiss deconvolution microscope (Carl Zeiss Pty. Ltd., Australasia) in brightfield mode and images were taken using a Zeiss AxioCam HR digital colour CCD camera (Carl Zeiss Pty. Ltd., Australasia). Adobe photoshop 2021 (22.1.1) was used to adjust the contrast and label all images.

Transmission electron microscopy

Uterine and placental tissues were cut into approximately 1 mm^3 portions and fixed in 2.5 % glutaraldehyde in 0.1 M phosphate buffer for 1 h. Tissue was then rinsed in 0.1 M phosphate buffer and fixed in 1% osmium tetroxide (OsO_4) in 0.1 M phosphate buffer at room temperature for 1 h. Samples were rinsed in 0.1 M phosphate buffer and then dehydrated in a series of ethanol. Ethanol was gradually replaced by Spurrs resin (Agar Scientific, Essex, UK) in 25% increments. Each piece of tissue was embedded in BEEM capsules and polymerised at 60 ˚C overnight. Resin blocks were removed from their capsules and ultrathin sections of approximately 70 nm were cut using a Ultracut S (Leica, Wetzlar, Germany) microtome with glass knives and placed on 200 mesh copper grids. At least three grids were made per resin block. Grids were post-stained with 2% uranyl acetate for 10 min and then rinsed with warm water. Grids were then post-stained with Reynold's lead citrate stain surrounded by sodium hydroxide pellets for 10 min and then rinsed in warm water. Grids were allowed to air dry and then sections were imaged with a FEI Tecnai T12 (FEI, USA) at 120 kV. The contrast was adjusted, and labels were added to all images using Adobe photoshop 2021 (22.1.1).

Scanning electron microscopy

Uterine and umbilical cord tissue was fixed in 2.5 % glutaraldehyde in 0.1 M phosphate buffer for 1 h. Tissue was then rinsed in 0.1 M phosphate buffer and fixed in 1 % osmium tetroxide (OsO_4) in 0.1M phosphate buffer at room temperature for 1 h. Samples were rinsed in 0.1 M Phosphate buffer and then gradually dehydrated in a series of ethanol, as for TEM tissue. Tissue was dried using a Leica EM CPD300 Critical Point Dryer (Leica, Wetzlar, Germany) with carbon dioxide as the drying agent. Dried tissue was then mounted onto aluminum stubs with a layer of carbon tape and coated with a 15 nm layer of gold. Images were captured with a Neoscope Tabletop SEM (JEOL Ltd, Japan). All images were processed and labelled using Adobe photoshop 2021 (22.1.1).

Results

Uterus of early pregnant *R. taylori* during the embryonic diapause period

The uterine wall of early pregnant *R. taylori* consists of a uterine epithelium, which is supported by a connective tissue layer and an outer muscular layer. (**Fig. 2 A**). Diapausing embryos are surrounded by a thin egg capsule, but do not occupy the entire capsule. The excess egg capsule is tightly coiled at one end of the uterus (**Fig. 2 A**). Tubular glands and blood vessels lie in the connective tissue layer (**Fig. 2 B, C**). Acidic (Alcian blue+) mucosubstances and periodic acid-Schiff+ substances are present in the lumen of the tubular glands (**Fig. 2 B**). The uterine epithelium is cuboidal and contacts the egg capsule in some uterine regions (**Fig. 2 D**). The cuboidal uterine epithelial cells have a high nucleus to cytoplasmic ratio, with few dark mitochondria in the cytoplasm (**Fig. 2 E**). Microplicae appear as elongated lateral folds on the apical surface of the uterine epithelial cells (**Fig. 2 F**).

Uterine and fetal tissues of late pregnant *R. taylori* during the placental period

The paraplacental uterine region

The columnar epithelial cells that cover the portion of the uterus not involved in placental formation have a domed shaped apical plasma membrane. The apical cytoplasm contains both periodic acid-Schiff+ substances and acidic mucosubstances (Alcian blue+; **Fig. 3 A**). The endothelial cells and the blood cells of the small blood vessels below the uterine epithelium are outlined by the periodic acid-Schiff+ stain (**Fig. 3 A**). Alkaline phosphatase enzyme activity is concentrated in the basal region of the uterine epithelium, in proximity to the blood vessels (**Fig. 3 B**). Acid phosphatase activity is concentrated in the apical portion of the uterine epithelium (**Fig. 3 C**). The control sections show no dark precipitate formation, which indicates no alkaline or acid phosphatase enzyme activity (**Fig 3 D, E**). Secretions are abundant on the surface of the columnar epithelial cells (**Fig 3 F**). The uterine epithelial cells have round basal nuclei and appear to release secretions into the uterine lumen (**Fig. 3 G, H**). Dilated intercellular spaces are prominent in some regions of the paraplacental uterine epithelium (**Fig 3. G, I**). The cytoplasm of the epithelial cells contains numerous secretory

vesicles, Golgi and lysosomes (**Fig. 3 G - L**). The microplicae on the luminal surface of the uterine epithelial cells are branched and appear to release round secretions. (**Fig. 3 J, K, L**).

The umbilical cord

The proximal portion of the yolk sac is connected to the embryo by an umbilical cord (**Fig. 4 A).** Numerous extensions termed appendiculae branch off the umbilical cord (**Fig. 4 A, B**). The umbilical cord consists of a vitelline artery, duct and vein (**Fig 4 B**). Periodic acid-Schiff+ substances are present on the apical surface of the cuboidal epithelial cells of the appendiculae (**Fig. 4 C**). Blood vessels occur in the connective tissue of the appendiculae (**data not shown).** The surface of most of the epithelial cells of the appendiculae are densely covered in microvilli (**Fig. 4 D**). Large domed secretory vesicles occur on the surface of some appendiculae epithelial cells (**Fig. 4 D).** The tubular glands present in the uterus of early pregnant females (**Fig. 2 D)** are also present in late pregnant females (**Fig. 4 E**). These glands contain acidic (Alcian Blue+) and periodic acid-Schiff+ substances (**Fig. 4 E**).

The placental interface

The uterine tissue forms highly branched villi that interdigitate with the fetal yolk sac (**Fig. 4 F**). The egg capsule adheres to the yolk sac and separates the fetal yolk sac from the uterine villi (**Fig. 4 G, H**). Numerous maternal and fetal blood vessels are near the respective uterine and yolk sac epithelial surface (**Fig. 4 G**). Periodic acid-Schiff+ substances are abundant in the lumen of the fetal yolk sac (**Fig. 4 H**). Alkaline phosphatase enzyme activity is concentrated in the uterine villi of the placenta (**Fig. 4 I**). Acid phosphatase enzyme activity occurs at the placental interface (**Fig. 4 J**) but is less prominent than in the paraplacental uterine regions (**Fig. 3 D**). The lack of dark precipitate formation in the control sections indicates no alkaline or acid phosphatase activity (**Fig. 4 K, L**).

The epithelium covering the uterine villi is low cuboidal and much thinner than the tall columnar uterine epithelium covering the paraplacental uterus (**Fig. 5**). In some areas, there is space between the egg capsule and the uterine epithelium, which may be an artefact of fixation and processing (**Fig. 5**). The uterine epithelial cells appear to produce secretions by the merocrine process (**Fig. 5 A**). Short, sparse microvilli cover the surface of some squamous uterine epithelial cells (**Fig. 5 B, C, D**). Secretions appear in the space between the

uterine epithelium and the egg capsule (**Fig. 5 C).** The lateral plasma membrane between the uterine epithelial cells are highly folded and numerous secretory vesicles and Golgi occur in the cytoplasm (**Fig. 5 D, E**). Mitochondria, lysosomes, pinocytotic vesicles and free ribosomes occur in the cytoplasm of the yolk sac ectodermal cells (**Fig. 5 F, G, H**). Endocytosed vesicles occur in the apical portion of the yolk sac ectodermal cells (**Fig. 5 G, H)**. In some areas, the ectodermal cell layer beneath the egg capsule is extremely thin (**Fig. 5 H**).

Invaginations along the basal lamina that separates the uterine epithelial cells from the underlying maternal blood vessels resemble caveolae (**Fig. 6 A, B**). These caveolae are also present along the basal and luminal plasma membrane of the yolk sac ectodermal cells and the endothelial cells of the fetal blood vessels (**Fig. 6 C, D**).

In other regions of the placental interface, the maternal and fetal blood vessels are separated by extremely attenuated uterine and yolk sac tissues (**Fig 7**). Fetal blood vessels occur in between the yolk sac ectoderm and endoderm cell layers (**Fig. 7 A, B).** The cytoplasm of the yolk sac cell ectodermal and endodermal cell layer is highly vacuolated (**Fig. 7 A, B**). Leukocytes and erythrocytes occur in the maternal blood vessels (**Fig. 7 C**). The diffusion distance between fetal and maternal blood vessels is between 2.5 – 1.5 µm in some regions (**Fig. 7 D, E, F**).

Discussion

The uterus of *Rhizoprionodon taylori* undergoes significant modifications during pregnancy. In the embryonic diapause period, the uterine epithelium is cuboidal, and the lack of cellular organelles suggests these cells are non-secretory. By late pregnancy, paraplacental areas not directly involved in placenta formation are columnar and appear to release secretions by the apocrine process, whilst the placenta consists of extensively branched uterine villi that interdigitate with the fetal yolk sac so strongly that the maternal and fetal tissues are impossible to separate without fine-scale dissection under a microscope. This complex interdigitation of fetal and maternal tissue increases the surface area available for fetomaternal exchange and is similar to the placental structure of most other sharks (*Rhizoprionodon terraenovae,* [21]; *Iago omanensis,* [22]*, Mustelus canis,* [7]*, Sphryna tiburo,*[11]*; Carcharhinus acronotus,* [23] and *Carcharhinus plumbeus;* [13] [24])*.* In all species studied so far, including *R. taylori,* the fetal yolk sac does not invade through the uterine mucosa during placental formation [7]. Hence, oxygen and nutrients from the maternal circulation must cross five layers to reach the fetal blood stream: the maternal capillary endothelium, the uterine epithelium, the embryonic egg capsule, the fetal yolk sac ectoderm and the fetal capillary endothelium. Shark placental structure is therefore similar to some amniote epitheliochorial placentae, in which maternal and embryonic tissues remain intact [2,25].

Even though we observed complex placental interdigitations, we found no evidence of erosion or absence of the egg capsule between the maternal and fetal tissues at any stage of pregnancy. Some viviparous squamates (snakes and lizards) retain a shell membrane between fetal and maternal tissues throughout pregnancy [26,27] but*,* in contrast to *R. taylori,* the shell membrane is often shed or absent in the placental regions that are involved in nutrient transport in viviparous squamates [27]. The uterine epithelial cells at the placental interface of *R. taylori* have cellular organelles that suggest a secretory function, and the opposing fetal yolk sac ectodermal cells that adhere to the embryonic egg capsule appear to absorb these secretions by endocytosis, suggesting that uterine secretions are released into the space between the placental uterine epithelium, transported through the embryonic egg capsule, and absorbed by the yolk sac ectoderm.

This placental structure supports the hypothesis that shark placental nutrient transport is by histotrophic uterine secretion followed by fetal absorption [7]. However, specialisations for hemotrophic placental transport of respiratory gases, water, wastes and potentially small organic nutrients are pronounced in placental regions where fetal and maternal blood vessels are extremely close. Hence, placental transport between uterine and fetal yolk sac tissues likely involves both hemotrophic and histotrophic mechanisms in *R. taylori*.

Uterine morphology during embryonic diapause

The lack of smooth endoplasmic reticulum and Golgi in the uterine epithelial cells during embryonic diapause suggests that there is no secretion by these cells while embryos are in diapause. However, PAS-positive material and acidic mucosubstances are present inside tubular-like uterine glands. Similar tubular glands have been described in the uterus of other placental sharks including *R. acutus, R. oligolinx, R. terraenovae, Scoliodon laticaudus* and *Carcharhinus plumbeus* [16,21,28,29]. Secretions from these glands may contribute to embryonic nutrition during pregnancy [28]. The presence of glandular secretions during the embryonic diapause period, when there is no embryonic growth, suggests that nutritive secretions may accumulate in the uterine fluid prior to the embryonic growth in *R. taylori* or that these glandular secretions have other functions.

All viviparous sharks, including *R. taylori,* are initially lecithotrophic [4,30]. In lecithotrophic sharks that do not supply embryos with non-yolk nutrients at any stage of pregnancy, uterine secretions may still lubricate and protect the uterine wall from abrasion by the developing embryos [7,31,32]. Alcian blue stains the acidic mucus layer on the luminal surface of the uterine epithelium of the lecithotrophic shark, *Orectolobus ornatus* [32]. Acidic alcian blue positive cells are more prevalent than positive periodic acid-Schiff cells in the uterine glands of early and late pregnant *R. taylori* females. Thus, the secretions from the glands in the uterine wall of early pregnant *R. taylori* could have similar lubricative and protective functions suggested for lecithotrophic sharks. The secretions could also be involved in maintaining and controlling the embryonic diapause period [15,33]. Future work should determine if the uterine glandular secretions of early pregnant *R. taylori* contain cytokines, growth factors, or transcription factors like those involved in regulating embryonic diapause and development in mammals [34].

Paraplacental uterine morphology during late pregnancy

Paraplacental regions of the *R. taylori* uterus do not directly contact fetal tissues, but still show distinct morphological differences from the early pregnant uterus.

Intercellular spaces

Some paraplacental areas have uterine epithelial cells with few microvilli on the luminal surface, and prominent dilated intercellular spaces. Similar dilated intercellular spaces also occur in the uterine epithelium of the viviparous non-placental sharks *Squalus acanthias* [35], *Pristiophorus sp.* [7], *M. antarcticus* [36] and the paraplacental uterine epithelium of the placental shark, *Prionace glauca* [12]. Such dilated intercellular spaces characterise epithelia that allow for water to be absorbed from the lumen and into the underlying tissues [37,38]. Therefore, the dilated intercellular spaces in the paraplacental uterine epithelium of late pregnant *R. taylori* may function to facilitate the maintenance of osmotic pressure in the uterine lumen [12].

Secretory uterine epithelial cells

In other paraplacental regions, the epithelial cells protrude into the uterine lumen and are covered with abundant apical microvilli. In some regions, secretory vesicles appear to be released into the uterine lumen by microvilli on the apical surface of the cells. These secretions may provide embryos with nutrients and/or a lubricative mucus during late pregnancy [7]. Uterine secretions seem to be important for embryonic nourishment before placental development in other sharks, and a similar secretory epithelium covers the paraplacental uterine regions in *Mustelus griseus* and *R. terraenovae*; [39,40]. In *R. taylori*, embryonic growth increases after the nutrients in the yolk sac are consumed, and before a placental connection between fetal and maternal tissues is established (**Fig.1;** [14,16]. We predict that uterine secretions are ingested or absorbed by fetal tissues (see 'embryonic uptake of uterine secretions' section below) and support embryonic growth from the time embryos come out of diapause until the end of pregnancy.

Uterine histotrophic secretions in viviparous elasmobranchs vary in nutrient content [7]. Non-placental sharks such as *M. antarcticus* secrete uterine mucus that may be involved in

306 transporting water and some inorganic nutrients to developing embryos [7,36]. In contrast,
307 lipid-rich histotrophic secretion is characteristic of the specialised uterine villi
308 (trophonemata) in rays, and the uterine epithelium of the white shark, *Carcharodon*
309 *carcharias* [41,42]. The epithelial cells of both tissue types contain abundant large lipid
310 droplets that are secreted in the uterine lumen [41,42]. While we did not observe lipid
311 droplets in the paraplacental uterine regions of *R. taylori*, electron dense organelles are
312 concentrated in the apical portion of the cytoplasm of the uterine epithelial cells. Intense
313 acid phosphatase enzyme activity in the same apical position of the uterine epithelium
314 suggests that these organelles are lysosomes [17,20]. Lysosomes are abundant in the
315 uterine epithelial cells of the placenta of domestic pigs *(Sus scrofa domesticus;* [20] and
316 skinks (*Pseudemoia* sp.*;* [19]; *Chalcides ocellatus;* [43]) where they may be involved in
317 breaking down macromolecules into smaller proteins, sugars and amino acids for transfer to
318 the developing embryo [19,20]. Support for this hypothesis is provided by the upregulation
319 of lysosomal genes in the uterus of the viviparous skink, *C. ocellatus* during pregnancy [44].
320 Catabolism of maternally derived macromolecules is likely to be important for embryonic
321 nourishment during pregnancy in *R. taylori,* because the uterine secretions must pass
322 through an acellular egg capsule to reach fetal tissues (see 'embryonic uptake of uterine
323 secretions' section below). The presence of lysosomal genes in the paraplacental uterus of
324 *R. taylori* would support our morphological interpretation that the paraplacental uterus is
325 specialised for histotrophic nutrient transport to developing embryos [44].

326 Alkaline phosphatase activity is not associated with the apical secretory surface of *R. taylori*
327 paraplacental uterine regions. Unlike viviparous skinks [19] and rats [45], this enzyme is
328 therefore probably not involved in histotrophic secretion in this region. We instead
329 observed basal localisation of alkaline phosphatase activity, which might be associated with
330 the maternal capillaries that occur immediately beneath the paraplacental uterine
331 epithelium of late pregnant *R. taylori*.

332 <u>Embryonic uptake of paraplacental uterine secretions</u>

333 Embryos of *R. taylori* are completely enclosed in a thin acellular egg capsule throughout
334 gestation, even at the interdigitated placental interface. Therefore, any nutrient transport
335 from mother to embryos must occur via the egg capsule, but the permeability of this

structure is unknown. The egg capsule of placental *Mustelus canis* is permeable to molecules smaller than 5,000 Da, whilst in placental *Sphyrna tiburo*, solutes less than 1,355 Da diffuse across the egg capsule [46,47]. We predict that the egg capsule of *R. taylori* is similarly permeable to low molecular weight nutrients such as glucose and small amino and fatty acids. Determining the permeability of the egg capsule in *R. taylori* will help elucidate the potential role of secretions from the paraplacental uterine epithelium for embryonic nourishment during pregnancy.

Once uterine secretions pass through the egg capsule, developing *R. taylori* embryos may ingest uterine secretions through their mouth or they may be absorbed by fetal tissues. The fetal yolk stalk forms the umbilical cord and associated appendiculae, which are densely covered in microvilli (**Fig. 3**). It is likely that the microvilli create an increased surface area on the appendiculae for absorption of secretions released by the paraplacental uterine epithelium. This appendicular function has been suggested in other placental sharks including *R. terraenovae* and *Sphyrna tiburo* [11,24]. Secretory smooth-surfaced epithelial cells are interspersed between the absorptive epithelial cells, and fetal capillaries are present immediately beneath the epithelium of the appendiculae. Hence, in addition to absorption, the appendiculae of *R. taylori* are probably also involved in secretion and respiratory gas exchange during late pregnancy. Fetal secretions during mammalian pregnancy contain hormones, cytokines and growth factors, which can modify the physiology of the placenta and increase the supply of nutrients to developing embryos [48,49]. The presence of these factors in the secretions from the appendiculae of *R. taylori* would suggest that developing embryos can manipulate the maternal metabolism during pregnancy.

Morphology of the placenta

Uterine secretion at the placental interface

In some placental regions, the low cuboidal epithelial cells that cover the uterine villi have sparse apical microvilli and contain numerous secretory vesicles and Golgi apparati, suggestive of synthesis and secretion. Secretions are released into the space between the uterine epithelium and the embryonic egg capsule (**Fig. 5**), which is consistent with other

365 placental sharks and may provide shark embryos with nutrients. The mechanisms involved
366 in secreting molecules from the placental uterine epithelium differ from those in
367 paraplacental uterine epithelium because the placental uterine epithelium lacks lysosomes
368 and associated acid phosphatase enzyme activity. Amniotes have specific placental
369 transport mechanisms for different types of nutrients [50,51]. For example, water and
370 inorganic ions readily diffuse across the placenta, membrane bound transporters are
371 involved in glucose and amino acids transport, and larger macromolecules may be secreted
372 in vesicles for embryonic absorption [2]. Alkaline phosphatase enzyme is associated with
373 tissues primarily involved in glucose and/or lipid transport, including the uterine epithelium
374 that opposes the fetal yolk sac (omphaloplacenta) of viviparous skinks [19,52]. Alkaline
375 phosphatase is active in the placental uterine villi of *R. taylori* (**Fig. 4 I**). Hence, the placental
376 uterine epithelium of *R. taylori* may be specialised for transferring glucose and essential
377 fatty acids to developing embryos. This hypothesis should be tested using molecular
378 techniques to determine if the membrane bound transporters responsible for glucose (e.g.
379 GLUT 1-14) and lipid (e.g. FABP, LPLs) transfer in placental amniotes [50,51] are expressed
380 and localised to the placental uterine epithelium of *R. taylori.* If these transporters are only
381 located in placental uterine regions, then the placenta may be responsible for transporting
382 specific types of nutrients during pregnancy in *R. taylori*.

383 Secretions released by the uterine epithelial cells appear to be endocytosed by the yolk sac
384 ectodermal cells at the placental interface of *R. taylori*. Absorption of uterine secretions by
385 endocytosis occurs in other placental sharks including *C. plumbeus* and *R. terraenovae* [7].
386 Endocytosed vesicles may subsequently be digested by the lysosomes in the yolk sac
387 ectodermal cells of *R. taylori* and other placental sharks [10]. These lysosomes may explain
388 the sparse acid phosphatase enzyme activity we observed in the placenta of *R. taylori* (**Fig. 4**
389 **J**). Endocytosis of uterine secretions by the yolk sac occurs in eutherian mammals,
390 marsupials and viviparous reptiles [53–55]. Endocytic receptors (e.g. megalin and cubilin)
391 are involved in transporting nutrients through the yolk sac of rodents and have been
392 localised to the yolk sac and fetal cells of the placental villi of humans [56,57]. The presence
393 of these receptors in the yolk sac tissues of late pregnant *R. taylori* would support our
394 hypothesis that nutritive uterine secretions are endocytosed by the yolk sac ectodermal
395 cells at the placental interface of *R. taylori*.

Caveolae may also be involved in transporting molecules across the placenta of *R. taylori.* We observed these plasma membrane invaginations along the yolk sac ectodermal cells, the endothelial cells of the fetal and maternal capillaries and the basal plasma membrane of the placental uterine epithelial cells (**Fig. 5, 6**). Caveolae are present on a range of mammalian cell types and are particularly abundant in endothelial cells where they are involved in transporting molecules from the lumen of the blood vessel across endothelial cell membranes [58,59].During transcytosis, caveolae form and release vesicles from the plasma membrane that travel to the opposite side of the cell where they fuse with the plasma membrane and release the vesicular contents [60]. Other sharks (*R. terraenovae* and *C. plumebus)* also have caveolae on fetal and maternal membranes at the placental interface [7]. Hence, caveolae may be a common morphological feature required for placental transport of molecules across the cell layers that intervene between the fetal and maternal blood streams of shark placentae.

The placental interface of *R. taylori* lacks the paracrystalline whorl-like inclusions that are present in the yolk sac tissues at the placental interface of other placental sharks, *C. plumbeus* and *R. terraenovae* [24]. These whorl-like inclusions resemble yolk protein precursors in amphibians and teleosts and may be involved in nourishing placental sharks during late pregnancy [7]. The placenta of *R. taylori* also lacks the large round cells that are interpreted to be melanomacrophages, and the cells with horseshoe shaped nuclei, in the light micrographs of the placenta of *R. terraenovae* [21]. The horseshoe shaped nuclei cells may be involved in transporting nutrients containing (PAS+) substances, across the uterine epithelium to the fetal yolk sac tissues [21]. The abundance of (PAS+) material in the yolk sac tissue at the placental interface of *R. taylori* is consistent with placental hammerhead sharks (*Sphyrna lewini and Sphyrna zygaena*;[61]) and suggests that neutral mucosubstances and/or carbohydrate moieties are transported across the placenta of *R. taylori.* Differences in cellular structures between shark species may indicate that placental transport mechanisms are species specific, or that different stages of pregnancy were examined in each species. The litter size and the length of pregnancy can affect placental morphology and function in different species of mammals [50,62]. Since *R. taylori* is the only placental shark with a confirmed embryonic diapause period, it is plausible that this species requires unique placental structures to facilitate rapid embryonic growth in the final 3 to 4

months of pregnancy (**Fig. 1**). This hypothesis should be tested using molecular techniques to compare the mechanisms involved in nutrient transport across the placentae of closely related carcharhinid sharks with different reproductive strategies (e.g. *R. taylori* and *R. terraenovae*). Additionally, uterine and placental structures should be examined in *R. taylori* females just after the diapause period (October - November; **Fig.1)** and compared to the females in this study as well as other placental sharks.

Fetal and maternal capillaries at the placental interface

In some placental regions, fetal and maternal cell layers are attenuated with a diffusion distance between maternal and fetal blood vessels of less than 2 µm (**Fig. 6).** Fetal and maternal blood vessels are in close proximity at the placental interface of other sharks [63], but the distance between blood vessels has not been estimated in any other species. The smallest diffusion distances in the placental regions involved in respiratory gas exchange of amniotes is comparable to the distances estimated in this study for *R. taylori* [61,48,62–64]..

In non-placental viviparous dogfish sharks (*Squalus cf. mitsukurii and Squalus cubensis*), the diffusion distance between the endothelial cells of the maternal blood vessel and the epithelial surface of the uterine villi is ~20 µm [65]. Oxygen from the maternal blood stream diffuses across this distance into the uterine fluid [65]. This maternal oxygen in the uterine fluid is estimated to supply embryos with less than 15-30% of their total demand for oxygen during late pregnancy [65]. The remaining oxygen required for the development of the late-stage embryos is supplied by the seawater that is periodically exchanged with the uterine fluid during pregnancy [31,65]. There is no evidence for this process of uterine flushing during pregnancy in any placental shark [31,65]. Therefore, the closely associated fetal and maternal blood vessels at the placental interface of *R. taylori* likely provides a direct transport route for the diffusion of respiratory gases during pregnancy.

The close association of fetal and maternal blood vessels at the placental interface of *R. taylori* (**Fig. 6**) should also facilitate the diffusion of water, solutes, inorganic ions and potentially small organic molecules such as amino acids [2,27]. Placental transport of nutrients directly from maternal to fetal blood vessels involves specific membrane bound transporters in mammals and potentially some squamates [2,26,44,49]. Solute carrier genes

(SLCs) are a large family of membrane bound transporters involved in transporting amino acids across the placenta of eutherian mammals, and putatively in the viviparous skink, *P. entrecasteauxii* and male-pregnant seahorse *H. abdominalis* [50,66,67, 68]. Expression and localisation of these SLC transporters to the placental uterine epithelium of *R. taylori,* would support our hypothesis that small organic molecules like amino acids are directly transported between maternal and fetal blood streams at the placental interface of *R. taylori.*

In conclusion, the morphological specialisations described here suggest that the yolk sac placenta functions in respiratory gas exchange and nutrient transport in *R. taylori*. The paraplacental uterine epithelium is secretory, and morphologically and enzymatically distinct from the placental uterine epithelium. An understanding of the mechanisms involved in embryonic growth after the diapause period in *R. taylori* requires further studies to examine the different functional roles played by the placenta, the paraplacenta and the appendiculae through pregnancy.

While we did find morphological evidence for histotrophic placental nutrient transfer in *R. taylori*, hemotrophic transfer of at least small nutrients directly between fetal and maternal blood streams at the placental interface of *R. taylori* cannot be ruled out. The expression and localisation of transporter molecules to vascularised placental regions that are morphologically specialised for gas exchange would suggest that both respiratory gas exchange and nutrient transport occurs directly between maternal and fetal blood streams [27]. Morphological data from a range of additional shark species is required to elucidate the extent of uterine and placental diversity among sharks, and address hypotheses regarding placental evolution in sharks.

Acknowledgements

The authors thank Christopher Friesen, Joshua Kemsley, Madie Cooper, Steve Moore, Jessica Dudley and Amos Mapleston for their assistance collecting the animals used within this study. The authors acknowledge the facilities and the scientific and technical assistance of Microscopy Australia at the Australian Centre for Microscopy and Microanalysis at the University of Sydney, and the Bosch Institute at the University of Sydney. This research was supported by Australian Research Council Discovery Project Grant DP180103370 to Camilla M. Whittington, Michael B. Thompson, Christopher R. Murphy, and Colin A. Simpfendorfer, and a L'Oreal–UNESCO for Women in Science Fellowship to Camilla M. Whittington. Alice L. Buddle is supported by an Australian Research Training Program Scholarship and the Joyce W Vickery Scientific Research Fund.

Author contributions and conflicts of interest

Alice L. Buddle, James U. Van Dyke, Camilla M. Whittington and Colin A. Simpfendorfer collected the tissue of *R. taylori* used in this study. Alice L. Buddle carried out the light microscopy, enzyme histochemistry, electron microscopy, and wrote the manuscript. James U. Van Dyke, Michael B. Thompson, Colin A. Simpfendorfer, Christopher R. Murphy, Samson N. Dowland and Camilla M. Whittington contributed to experimental design, image interpretation, manuscript revisions and have seen and approved the final version. All authors have no conflict of interest to declare.

503 **References**

504 [1] D.G. Blackburn, Evolution of vertebrate viviparity and specializations for fetal
505 nutrition: a quantitative and qualitative analysis, J. Morphol. 276 (2015) 961–990.

506 [2] F.B.P. Wooding, G.J. Burton, Comparative placentation: structures, functions and
507 evolution, Springer-Verlag, Heidelberg, 2008.

508 [3] O.W. Griffith, G.P. Wagner, The placenta as a model for understanding the origin and
509 evolution of vertebrate organs, Nat. Ecol. Evol. 1 (2017) 1–10.
510 https://doi.org/10.1038/s41559-017-0072.

511 [4] C.L. Conrath, J.A. Musick, Reproductive biology of elasmobranchs, in: J. C. Carrier, J. A.
512 Musick, and M. R. Heithaus (Eds.), Biology of sharks and their relatives, second
513 edition, CRC Press, Boca Raton, FL, USA, 2012, pp. 291–306.

514 [5] J.P. Wourms, Viviparity: The maternal-fetal relationship in fishes, Integr. Comp. Biol.
515 21 (1981) 473–515. https://doi.org/10.1093/icb/21.2.473.

516 [6] W.C. Hamlett, J.P. Wourms, J. Hudson, Ultrastructure of the full-term shark yolk sac
517 placenta. I. Morphology and cellular transport at the fetal attachment site, J.
518 Ultrastruct. Res. 91 (1989) 192–206.

519 [7] W.C. Hamlett, G. Kormanik, M. Storrie, B. Stevens, T.I. Walker, Chondrichthyan parity,
520 lecithotrophy and matrotrophy, in: W.C. Hamlett (Ed.), Reproductive Biology and
521 Phylogeny of Chondrichthyes Sharks, Batoids Chimaeras, Science Publishers, Enfield,
522 NH, USA, 2005, pp. 395–434.

523 [8] A.L. Buddle, J.U. Van Dyke, M.B. Thompson, C.A. Simpfendorfer, C.M. Whittington,
524 Evolution of placentotrophy: using viviparous sharks as a model to understand
525 vertebrate placental evolution, Mar. Freshw. Res. 70 (2019).
526 https://doi.org/10.1071/MF18076.

527 [9] A.N. Ostrovsky, S. Lidgard, D.P. Gordon, T. Schwaha, G. Genikhovich, A. V. Ereskovsky,
528 Matrotrophy and placentation in invertebrates: a new paradigm, Biol. Rev. Camb.
529 Philos. Soc. 91 (2016) 673–711. https://doi.org/10.1111/brv.12189.

[10] W.C. Hamlett, A.M. Eulitt, J.R. Jarrell, M.A. Kelly, Uterogestation and placentation in elasmobranchs, J. Exp. Zool. 266 (1993) 347–367.

[11] D.A. Schlernitzauer, P.W. Gilbert, Placentation and associated aspects of gestation in the bonnethead shark, *Sphyrna tiburo*, J. Morphol. 120 (1966) 219–231. https://doi.org/10.1002/jmor.1051200302.

[12] T. Otake, K. Mizue, The fine structure of the intra-uterine epithelium during late gestation in the blue shark, *Prionace glauca*, Japanese J. Ichthyol. 33 (1986) 162–167. https://doi.org/10.1007/BF02905844.

[13] W.C. Hamlett, J.P. Wourms, J. Hudson, Ultrastructure of the full-term shark yolk sac placenta. III. The maternal attachment site., J. Ultrastruct. Res. 91 (1985) 221–231.

[14] C.A. Simpfendorfer, Reproductive strategy of the Australian sharpnose shark, *Rhizoprionodon taylori* (Elasmobranchii:Carcharhinidae), from cleveland bay, Northern Queensland, Mar. Freshw. Res. 43 (1992) 67–75. https://doi.org/10.1071/MF9920067.

[15] D. Waltrick, C. Awruch, C. Simpfendorfer, Embryonic diapause in the elasmobranchs, Rev. Fish Biol. Fish. 22 (2012) 849–859. https://doi.org/10.1007/s11160-012-9267-5.

[16] C.A. Simpfendorfer, The biology of sharks of the faimly Carcharhinidae from the nearshore waters of Cleveland Bay, with particular reference to *Rhizoprionodon taylori*, James Cook University, 1993.

[17] J.A. Kiernan, Histological and histochemical methods: theory and practice, fourth edition, Scion Publishing Limited, London, Ontario, Canada, 2008.

[18] G. Gomori, Microscopic histochemistry, principles and practice, University of Chicago Press, Chicago, 1952.

[19] J.M. Biazik, M.B. Thompson, C.R. Murphy, Lysosomal and alkaline phosphatase activity indicate macromolecule transport across the uterine epithelium in two viviparous skinks with complex placenta, J. Exp. Zool. 312 (2009) 817–826.

[20] V. Dantzer, An extensive lysosomal system in the maternal epithelium of the porcine placenta, Placenta. 5 (1984) 117–129.

[21] A.N. Haines, M.F. Flajnik, J.P. Wourms, Histology and immunology of the placenta in the Atlantic Sharpnose Shark, *Rhizoprionodon terraenovae*, Placenta. (2006) 1114–1123.

[22] L. Fishelson, A. Baranes, Observations on the Oman shark, *Iago omanensis* (Triakidae), with emphasis on the morphological and cytological changes of the oviduct and yolk sac during gestation, J. Morphol. 236 (1998) 151–165. https://doi.org/10.1002/(SICI)1097-4687(199806)236:3<151::AID-JMOR1>3.0.CO;2-6.

[23] W.C. Hamlett, Electron microscopic investigations of the fetal membranes and uterus in the blacknose shark, *Carcharhinus acronotus*, Anat. Rec. 226 (1990) 40a.

[24] W.C. Hamlett, Evolution and morphogenesis of the placenta in sharks, J. Exp. Zool. 252 (1989) 35–52.

[25] C.R. Murphy, Uterine receptivity and the plasma membrane transformation, Cell Res. 14 (2004) 259–267. https://doi.org/10.1038/sj.cr.7290227.

[26] J.R. Stewart, Placental structure and nutritional provision to embryos in predominantly lecithotrophic viviparous reptiles, Integr. Comp. Biol. 32 (1992) 303–312. https://doi.org/10.1093/icb/32.2.303.

[27] D.G. Blackburn, Viviparous placentotrophy in reptiles and the parent–offspring conflict, J. Exp. Zool. – B. Mol. Dev. Evol. 324 (2015) 532–548.

[28] G. Mahadevan, Preliminary observations on the structure of the uterus and the placenta of a few Indian elasmobranchs, Proc. Indian Acad. Sci. - Sect. B. 11 (1940) 1–44. https://doi.org/10.1007/BF03048096.

[29] A. Baranes, J. Wendling, The early stages of development in *Caracharhinus plumbeus,* J. Fish Biol. 18 (1981) 159–175.

[30] J.P. Wourms, Maximization of evolutionary trends for placental viviparity in the

spadenose shark, *Scoliodon laticaudus*, Environ. Biol. Fishes. 38 (1993) 269–294. https://doi.org/10.1007/978-94-017-3450-9_24.

[31] M.T. Ellis, N.M. Otway, Uterine fluid composition of the dwarf ornate wobbegong shark (*Orectolobus ornatus*) during gestation, Mar. Freshw. Res. 62 (2011) 576–582. https://doi.org/10.1071/MF10138.

[32] A.L. Buddle, N.M. Otway, J.U. Van Dyke, M.B. Thompson, C.R. Murphy, S.N. Dowland, C.A. Simpfendorfer, M.T. Ellis, C.M. Whittington, Structural changes to the uterus of the dwarf ornate wobbegong shark (*Orectolobus ornatus*) during pregnancy, J. Morphol. 281 (2020). https://doi.org/10.1002/jmor.21109.

[33] D. Waltrick, S.M. Jones, C.A. Simpfendorfer, C.A. Awruch, Endocrine control of embryonic diapause in the Australian sharpnose shark *Rhizoprionodon taylori,* PLoS One. 9 (2014). https://doi.org/10.1371/journal.pone.0101234.

[34] M.B. Renfree, J.C. Fenelon, The enigma of embryonic diapause, Dev. 144 (2017) 3199–3210. https://doi.org/10.1242/dev.148213.

[35] W.P. Jollie, L.G. Jollie, Electron microscopic observations on accommodations to pregnancy in the uterus of the spiny dogfish, *Squalus acanthias*, J. Ultrasructure Res. 20 (1967) 161–178. https://doi.org/10.1016/S0022-5320(67)90279-1.

[36] M.T. Storrie, T.I. Walker, L.J. Laurenson, W.C. Hamlett, Gestational morphogenesis of the uterine epithelium of the gummy shark (*Mustelus antarcticus*), J. Morphol. 270 (2009) 319–336. https://doi.org/10.1002/jmor.10693.

[37] G.I. Kaye, H.O. Wheeler, R.T. Whitlock, N. Lane, Fluid transport in the rabbit gallbladder. A combined physiological and electron microscopic study, J. Cell Biol. 30 (1966) 237–268. https://doi.org/10.1083/jcb.30.2.237.

[38] J.M. Whittamore, Osmoregulation and epithelial water transport: Lessons from the intestine of marine teleost fish, J. Comp. Physiol. B Biochem. Syst. Environ. Physiol. 182 (2012) 1–39. https://doi.org/10.1007/s00360-011-0601-3.

[39] T. Otake, Classification of Reproductive Modes in Sharks with Comments on Female

609 Reproductive Tissues and Structures, in: H.L. Pratt, S.H. Gruber, Jr, T. Taniuchi (Eds.),
610 Elasmobranchs as Living Resources, Adv. Biol. Ecol. Syst. Status Fish., NOAA, US
611 Department of Commerce, 1990: pp. 111–130.

612 [40] J.I. Castro, J.P. Wourms, Reproduction, placentation, and embryonic development of
613 the Atlantic sharpnose shark, *Rhizoprionodon terraenovae*, J. Morphol. 218 (1993)
614 257–280. https://doi.org/10.1002/jmor.1052180304.

615 [41] W.C. Hamlett, J.A. Musick, A.M. Eulitt, R.L. Jarrell, M.A. Kelly, Ultrastructure of uterine
616 trophonemata, accommodation for uterolactation, and gas exchange in the southern
617 stingray, *Dasyatis americana,* Can. J. Zool. 74 (1996) 1417–1430.

618 [42] K. Sato, M. Nakamura, T. Tomita, M. Toda, K. Miyamoto, R. Nozu, How great white
619 sharks nourish their embryos to a large size: Evidence of lipid histotrophy in lamnoid
620 shark reproduction, Biol. Open. 5 (2016) 1211–1215.
621 https://doi.org/10.1242/bio.017939.

622 [43] G. Corso, G.M. Delitala, M. Carcupino, Uterine morphology during the annual cycle in
623 *Chalcides ocellatus tiligugu* (Gmelin) (Squamata: Scincidae), J. Morphol. (2000) 153–
624 165.

625 [44] M.C. Brandley, R.L. Young, D.L. Warren, M.B. Thompson, G.P. Wagner, Uterine gene
626 expression in the live-bearing lizard, *Chalcides ocellatus*, reveals convergence of
627 squamate reptile and mammalian pregnancy mechanisms, Genome Biol. Evol. 4
628 (2012) 394–411. https://doi.org/10.1093/gbe/evs013.

629 [45] M. Bucci, C.R. Murphy, Alkaline phosphatase distribution in the plasma membrane of
630 uterine epithelial cells is markedly altered during early pregnancy in the rat, Cell Biol.
631 Int. 19 (1995) 921–928. https://doi.org/10.1006/cbir.1995.1030.

632 [46] J. Lombardi, T. Files, Egg capsule structure and permeability in the viviparous shark,
633 *Mustelus canis,* J. Exp. Zool. 267 (1993) 76–85.
634 https://doi.org/10.1002/jez.1402670111.

635 [47] T.C.K. Heiden, A.N. Haines, C. Manire, J. Lombardi, T.J. Koob, Structure and

permeability of the egg capsule of the bonnethead shark, *Sphyrna tiburo*, J. Exp. Zool. –A. Comp. Exp. Biol. 303A (2005) 577–589.

[48] B. Crespi, C. Semeniuk, Parent–offspring conflict in the evolution of vertebrate reproductive mode, Am. Nat. 163 (2004) 635–653.

[49] A.L. Fowden, J.W. Ward, F.P.B. Wooding, A.J. Forhead, M. Constancia, Programming placental nutrient transport capacity, J. Physiol. 572 (2006) 5–15.

[50] A.M. Carter, Evolution of placental function in mammals: the molecular basis of gas and nutrient transfer, hormone secretion, and immune responses, Physiol. Rev. 92 (2012) 1543–1576.

[51] J.U. Van Dyke, M.C. Brandley, M.B. Thompson, The evolution of viviparity: molecular and genomic data from squamate reptiles advance understanding of live birth in amniotes, Reproduction. 147 (2014) R15–R26. https://doi.org/10.1530/REP-13-0309.

[52] J.F. Danielli, Phosphatases and other enzymes considered in relation to active transport and the functions of fibrous protein structures., Proc. R. Soc. Lond. B. Biol. Sci. 142 (1954) 146–154. https://doi.org/10.1098/rspb.1954.0013.

[53] B.F. King, A.C. Enders, The fine structure of the guinea pig visceral yolk sac placenta, Am. J. Anat. 127 (1970) 397–413. https://doi.org/10.1002/aja.1001270405.

[54] J.R. Stewart, Yolk sac placentation in reptiles: structural innovation in a fundamental vertebrate fetal nutritional system, J. Exp. Zool. 266 (1993) 431–449. https://doi.org/10.1002/jez.1402660509.

[55] K. Ferner, A. Mess, Evolution and development of fetal membranes and placentation in amniote vertebrates, Respir. Physiol. Neurobiol. 178 (2011) 39–50.

[56] I.E. Zohn, A.A. Sarkar, The visceral yolk sac endoderm provides for absorption of nutrients to the embryo during neurulation, Birth Defects Res. Part A - Clin. Mol. Teratol. 88 (2010) 593–600. https://doi.org/10.1002/bdra.20705.

[57] K.A. Burke, E. Jauniaux, G.J. Burton, T. Cindrova-Davies, Expression and

662 immunolocalisation of the endocytic receptors megalin and cubilin in the human yolk
663 sac and placenta across gestation, Placenta. 34 (2013) 1105–1109.

664 [58] R.G. Anderson, The caveolae membrane system, Annu. Rev. Biochem. 67 (1998) 199–
665 225.

666 [59] R.J. Madawala, C.E. Poon, S.N. Dowland, C.R. Murphy, PTRF is associated with
667 caveolin 1 at the time of receptivity: but SDPR is absent at the same time, Histochem.
668 Cell Biol. 143 (2015) 637–644. https://doi.org/10.1007/s00418-015-1308-4.

669 [60] S.A. Predescu, D.N. Predescu, A.B. Malik, Molecular determinants of endothelial
670 transcytosis and their role in endothelial permeability, Am. J. Physiol. - Lung Cell. Mol.
671 Physiol. 293 (2007). https://doi.org/10.1152/ajplung.00436.2006.

672 [61] H. Soma, N. Murai, K. Tanaka, T. Oguro, H. Kokuba, I. Yoshihama, K. Fujita, S. Mineo,
673 M. Toda, S. Uchida, T. Mogoe, Review: Exploration of placentation from human
674 beings to ocean-living species, Placenta, 2013.
675 https://doi.org/10.1016/j.placenta.2012.11.021.

676 [62] I. Capellini, C. Venditti, R.A. Barton, Placentation and maternal investment in
677 mammals, Am. Nat. 177 (2011) 86–98.

678 [63] W.C. Hamlett, Evolution and morphogenesis of the placenta in sharks, J. Exp. Zool.
679 252 (1989) 35–52. https://doi.org/10.1002/jez.1402520406.

680 [64] D.G. Blackburn, R.L. Lorenz, Placentation in garter snakes. II. Transmission EM of the
681 chorioallantoic placenta of *Thamnophis radix* and *T. sirtalis*, J. Morphol. (2003).
682 https://doi.org/10.1002/jmor.10083.

683 [65] T. Tomita, C.F. Cotton, M. Toda, Ultrasound and physical models shed light on the
684 respiratory system of embryonic dogfishes, Zoology. 119 (2016) 36–41.
685 https://doi.org/10.1016/j.zool.2015.09.002.

686 [66] O.W. Griffith, M.C. Brandley, K. Belov, M.B. Thompson, Reptile pregnancy is
687 underpinned by complex changes in uterine gene expression: A comparative analysis
688 of the uterine transcriptome in viviparous and oviparous lizards, Genome Biol. Evol. 8

689 (2016) 3226– 3239.

690 [67] C.M. Whittington, O.W. Griffith, W. Qi, M.B. Thompson, A.B. Wilson, Seahorse brood
691 pouch transcriptome reveals common genes associated with vertebrate pregnancy,
692 Mol. Biol. Evol. (2015). https://doi.org/10.1093/molbev/msv177.

693 [68] J.U. Van Dyke, O.W. Griffith, Mechanisms of reproductive allocation as drivers of
694 developmental plasticity in reptiles, J. Exp. Zool. Part A Ecol. Integr. Physiol. 329
695 (2018) 275–286. https://doi.org/10.1002/jez.2165.

696

Figure 1. Schematic diagram of embryonic development in *Rhizoprionodon taylori.* Females mate and their eggs are fertilised shortly after they give birth in January. Fertilised eggs (light grey) are surrounded by an egg capsule (dark grey). Embryonic growth is suspended at the blastodisc stage for the first seven months of pregnancy (Feb – end of Aug). During this embryonic diapause period, the egg capsule is coiled in the anterior portion of the uterus. Embryos begin to slowly grow in late August. Developing embryos are initially reliant on nutrients contained in the yolk sac. Once the nutrients in the yolk sac have been consumed, the yolk sac forms the embryonic portion of the placenta (red) and the yolk stalk forms the umbilical cord (light pink). The umbilical cord is covered by outgrowths termed appendiculae (light pink). In late pregnancy, the egg capsule is thin and stretches around the entire embryo (black) and the yolk sac portion of the placenta (red). Embryos reach full-term (200mm-250mm) in mid-January.

Figure 2. Light and electron micrographs of the uterus of *R. taylori* during the embryonic diapause period. **A, B**) Uterine wall and egg capsule stained by the combined Alcian blue (AB)/periodic acid-Schiff (PAS) procedure: purple indicates neutral mucosubstances; blue indicates acidic mucosubstances. **C, D)** Uterine glands and uterine epithelium stained with hematoxylin and eosin. **E)** Transmission electron micrograph of the cuboidal uterine epithelium. **F**) Scanning electron micrograph of the microplicae on the surface of the uterine epithelium. Blood vessels (asterisk), connective tissue (CT), egg capsule (EC and black arrows), glandular lumen (arrowheads), microplicae (white arrows), mitochondria (m), muscle (M), nucleus (N), tubular-like glands (G), uterine epithelium (UE) and uterine lumen (L).

Fig 3. Light and transmission electron micrographs of the paraplacental uterine epithelium of *R. taylori* during the placental late pregnancy period. **A**) The columnar uterine epithelium stained by the combined Alcian blue (AB)/periodic acid-Schiff (PAS) procedure. Both neutral mucosubstances (Periodic acid-Schiff+) and acidic mucosubstances (alcian blue+) are present. **B**) Dark brown basal staining of the uterine epithelium (UE) indicates alkaline phosphatase activity. **C**) Black deposits in the apical region of the uterine epithelium indicates acid phosphatase activity. **D**) Control sections of paraplacental uterine tissue showing no alkaline phosphatase enzyme activity and **E**) no acid phosphatase enzyme

activity. **F**) Scanning electron micrograph showing secretions on the surface of the uterine epithelium. **G- L**) Transmission electron micrographs of the paraplacental uterine epithelium. Connective tissue (CT), Golgi (G), intercellular space (ICS), lysosomes (ly), microplicae (mp), nucleus (N), secretions (asterisk), secretory vesicles (sv), uterine epithelium (UE), uterine lumen (L).

Figure 4. The placenta in late pregnant *Rhizoprionodon taylori.* **A)** Schematic diagram of the umbilical cord and placenta from Buddle *et al.,* 2018. The umbilical cord has outgrowths termed 'appendiculae' and attaches the proximal portion of the fetal yolk sac to the embryo. **B)** Hematoxylin and eosin stained cross section through umbilical cord. **C)** The epithelium (AE) and connective tissue core (CT) of the appendiculae stained with Periodic acid-Schiff: purple indicates neutral mucosubstances. **D**) Scanning electron micrograph of the microvilli (m), secretions (s) on the surface of the appendiculae epithelial cells. **E**) Tubular glands (G) in the uterine connective tissue (CT) stained with the combined Alcian blue (AB)/periodic acid-Schiff (PAS) procedure. **F**) Light micrograph of a cross section through the placenta of late pregnant *R. taylori.* The uterine villi that interdigitate with the fetal yolk sac are outlined in red. **G)** Placental interface stained with hematoxylin and eosin, **H**) periodic acid-Schiff (PAS), **I**) alkaline phosphatase enzyme and **J**) acid phosphatase enzyme. **K**) Control sections of placental interface showing no alkaline phosphatase enzyme activity and **L**) no acid phosphatase enzyme activity. Appendiculae (A), appendiculae epithelium (AE), connective tissue (CT), egg capsule (arrows), fetal blood vessel (FBV), maternal blood vessel (MBV), microvilli (m), periodic acid-Schiff material (asterisk), secretions (s), tubular-like gland (G), uterine villi (V), vitelline artery (VA), vitelline duct (D), vitelline vein (VV), yolk sac tissue (Y).

Figure 5. Transmission electron micrographs of the placental interface between the yolk sac and the uterine epithelium of *R. taylori.* Egg capsule (EC); endocytosed vesicles (white arrowheads); fetal blood vessels (FBV); free ribosomes (RIB); Golgi (G); leukocytes (Lu); lysosomes (Ly); maternal blood vessels (MBV); microvilli (mv); mitochondria (m); pinocytotic vesicles (circle); plasma membrane (arrows); secretions (asterisks); secretory vesicles (sv); uterine epithelium (UE); yolk sac ectoderm (ECT).

Figure 6. Transmission electron micrographs of the caveolae on the uterine epithelial cells, the endothelial cells of the maternal blood vessels, the fetal yolk sac cells and the

endothelial cells of the fetal blood vessels at the placental interface of *R. taylori.* Caveolae (arrows); egg capsule (black arrowheads); endocytosed vesicles (white arrowheads); fetal blood vessel (FBV); Golgi (G); maternal blood vessel (MBV); uterine epithelium (UE); yolk sac ectoderm (ECT).

Figure 7. Transmission electron micrographs of closely apposed fetal and maternal blood vessels at the placental interface of *R. taylori.* The diffusion distance between these fetal and maternal blood vessels is approximately 1.5 – 2.5 µm. Egg capsule (EC); endothelial cell (EN); fetal blood vessel (FBV); leukocyte (Lu); maternal blood vessel (MBV); uterine epithelium (UE); yolk sac ectodermal cell layer (ECT); yolk sac endodermal cell layer (END).

Figure 1

Click here to access/download;Figure;Figure 1. R. taylori embryonic development figure.pdf

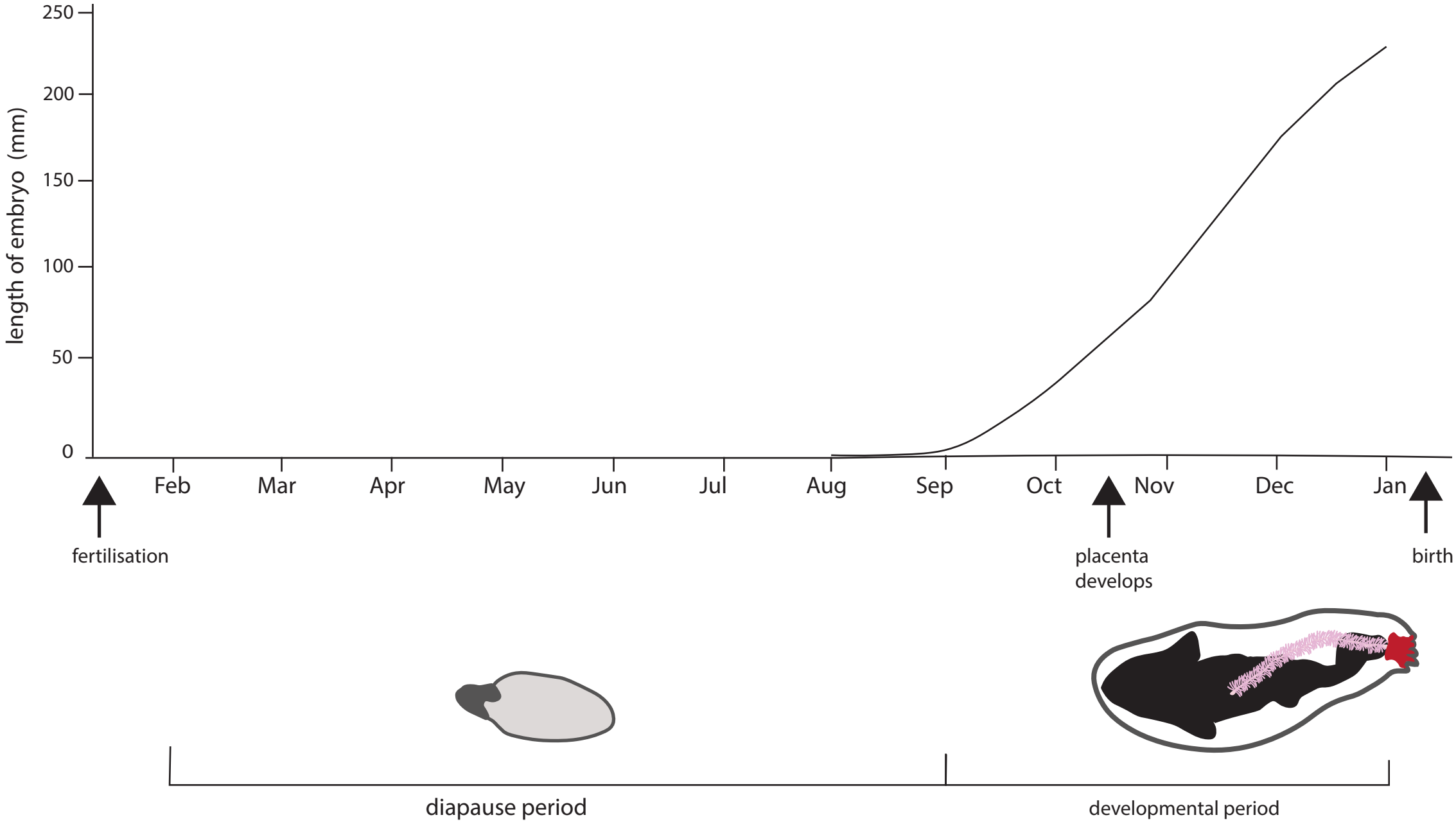

Figure 2

Click here to access/download;Figure;Figure 2_Early preg uterus .pdf

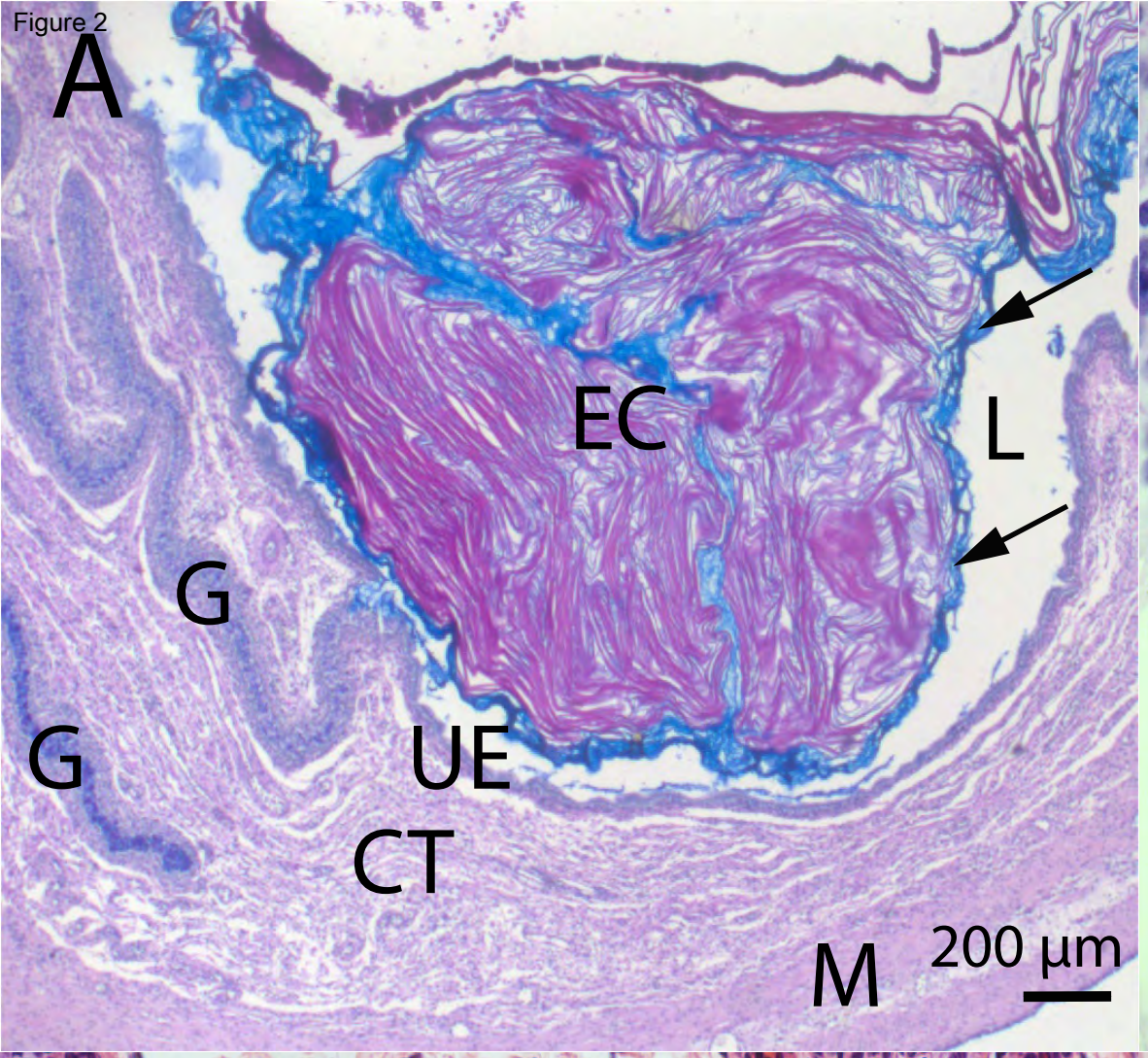

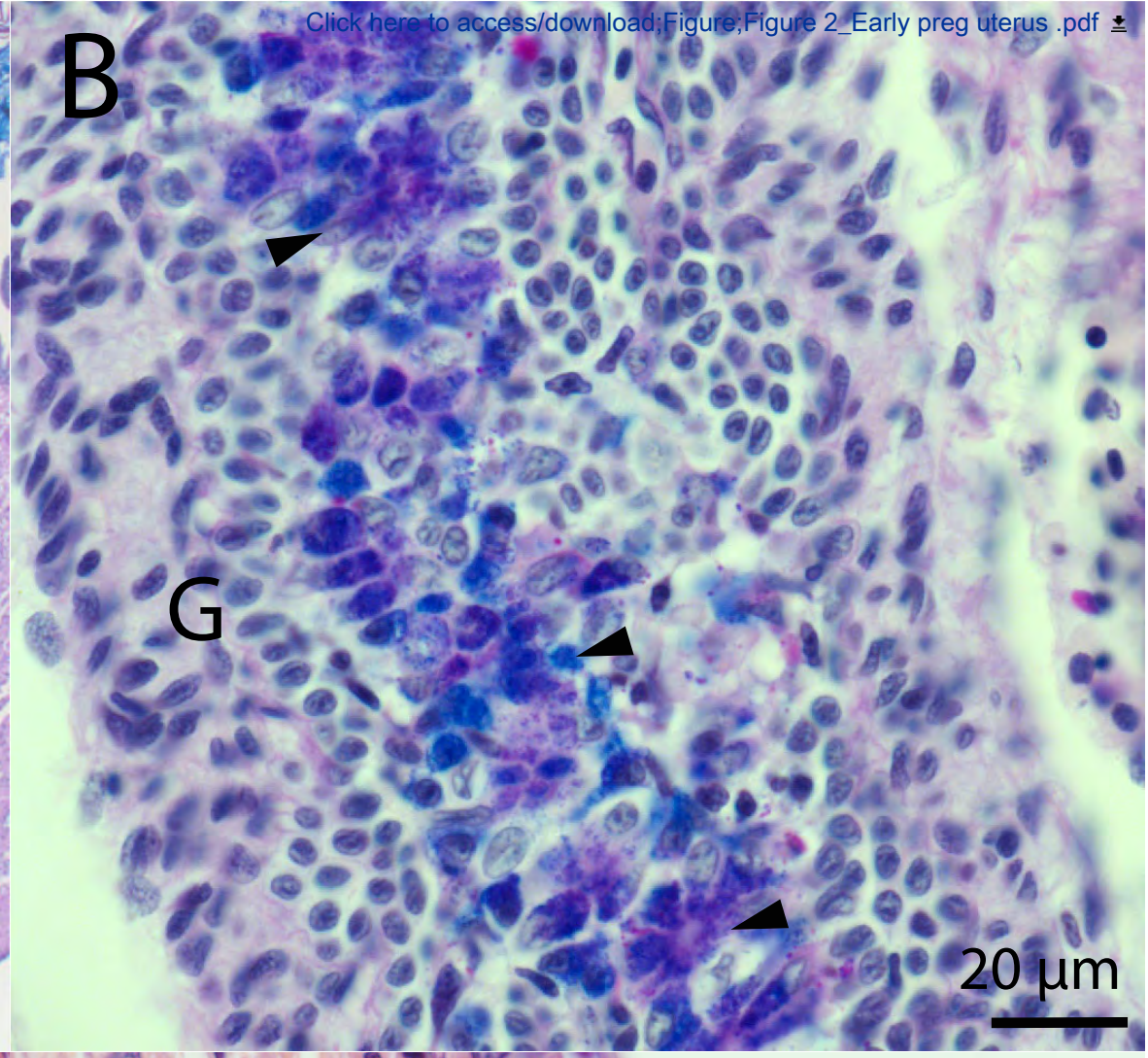

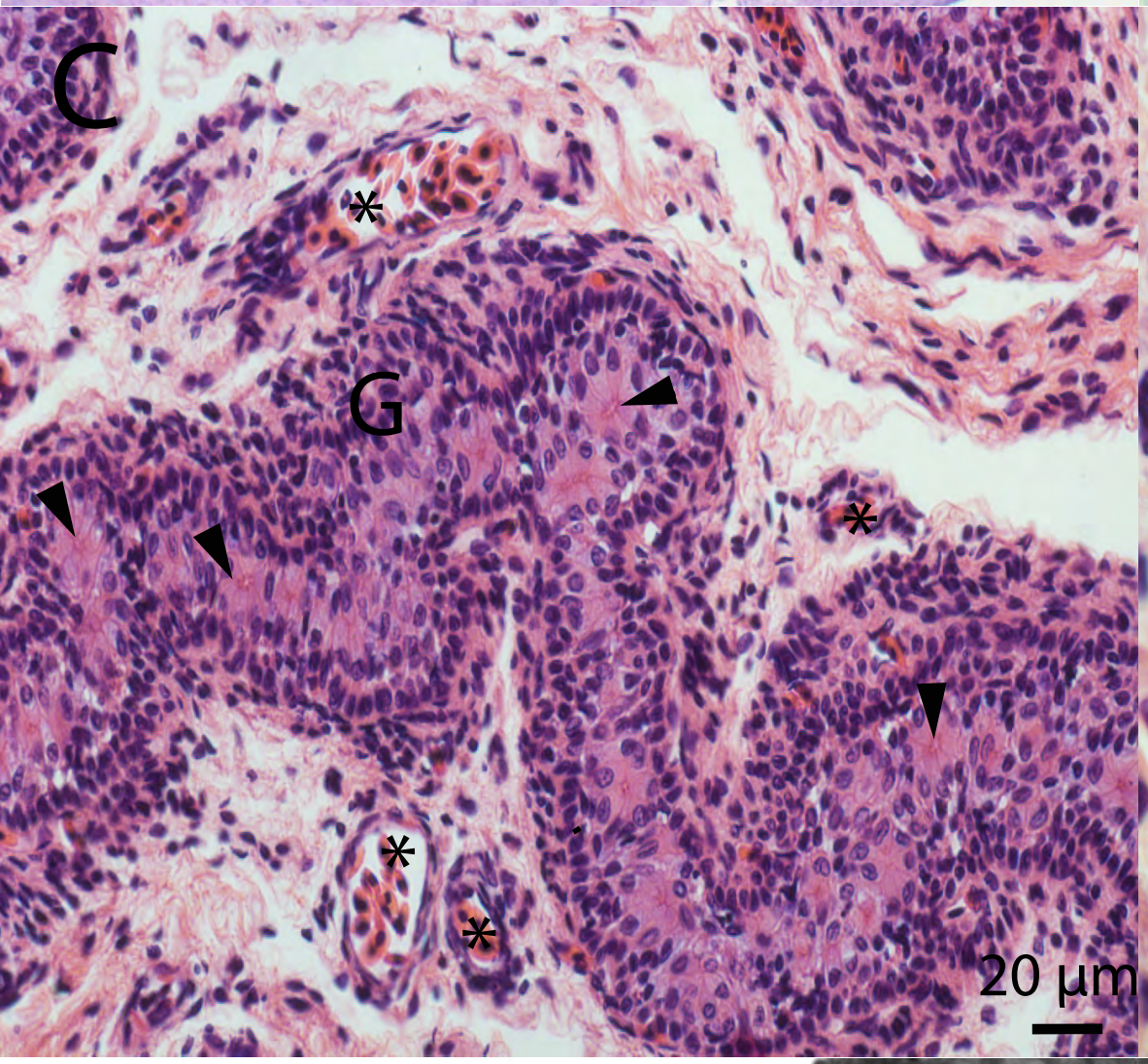

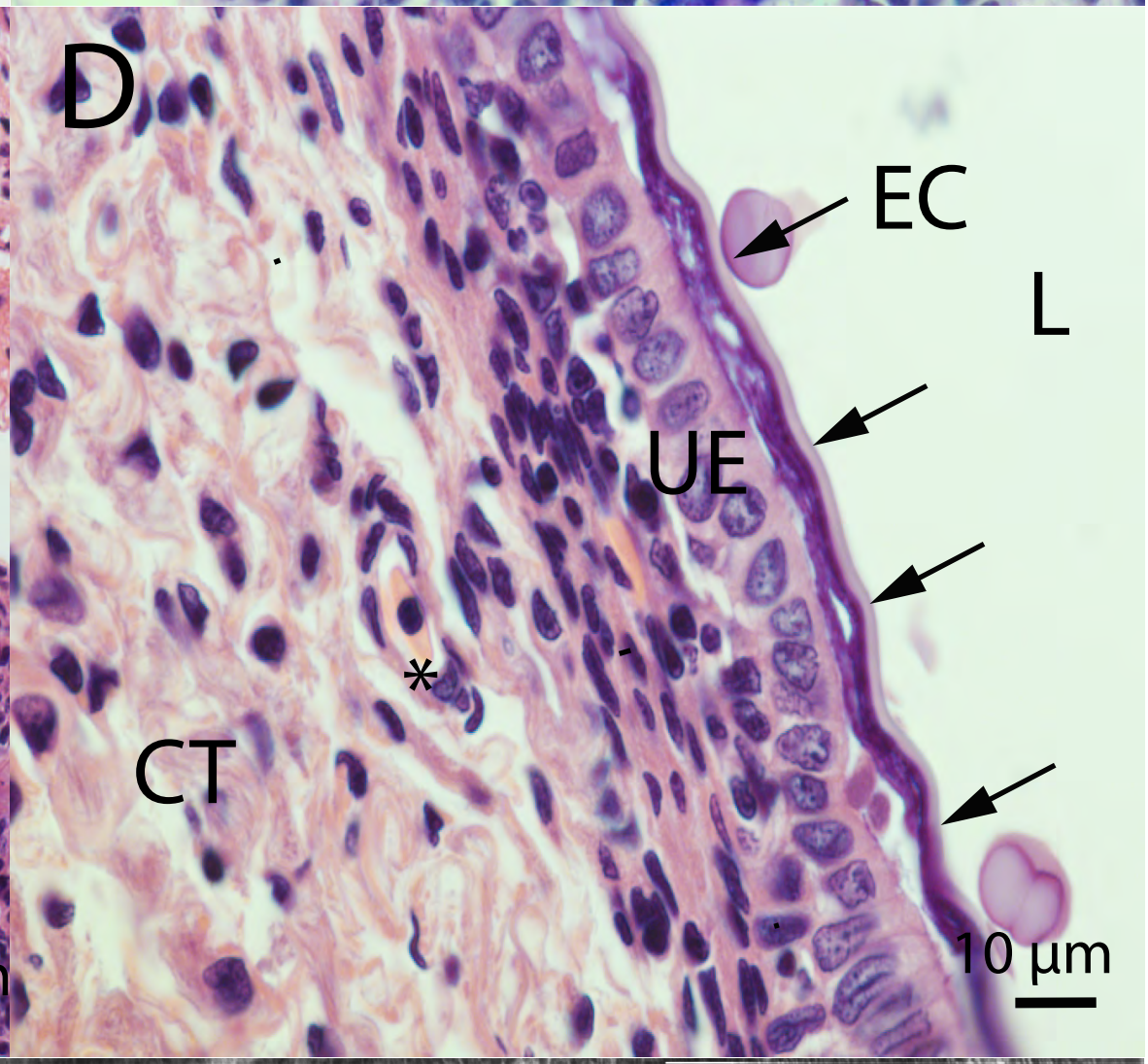

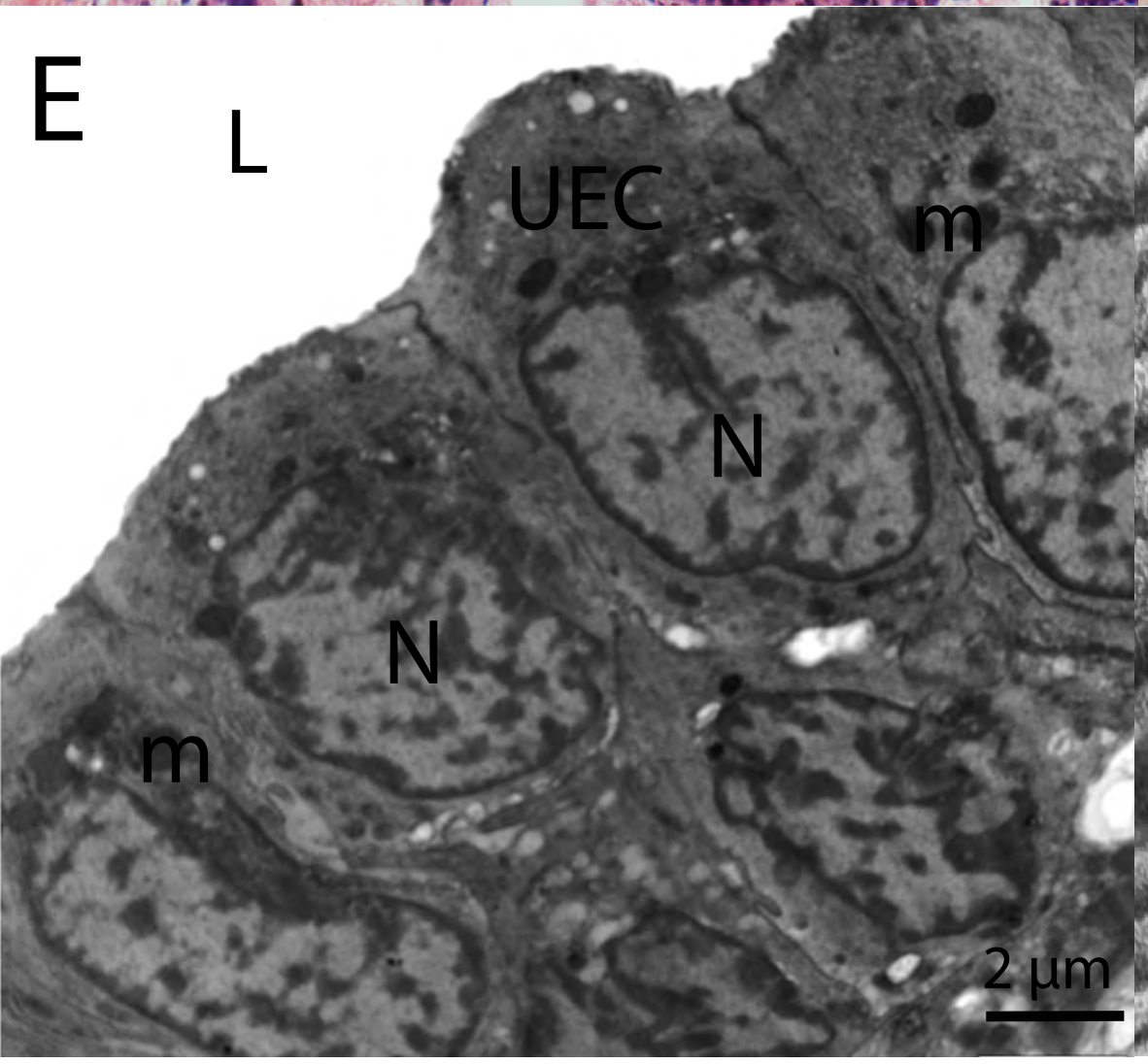

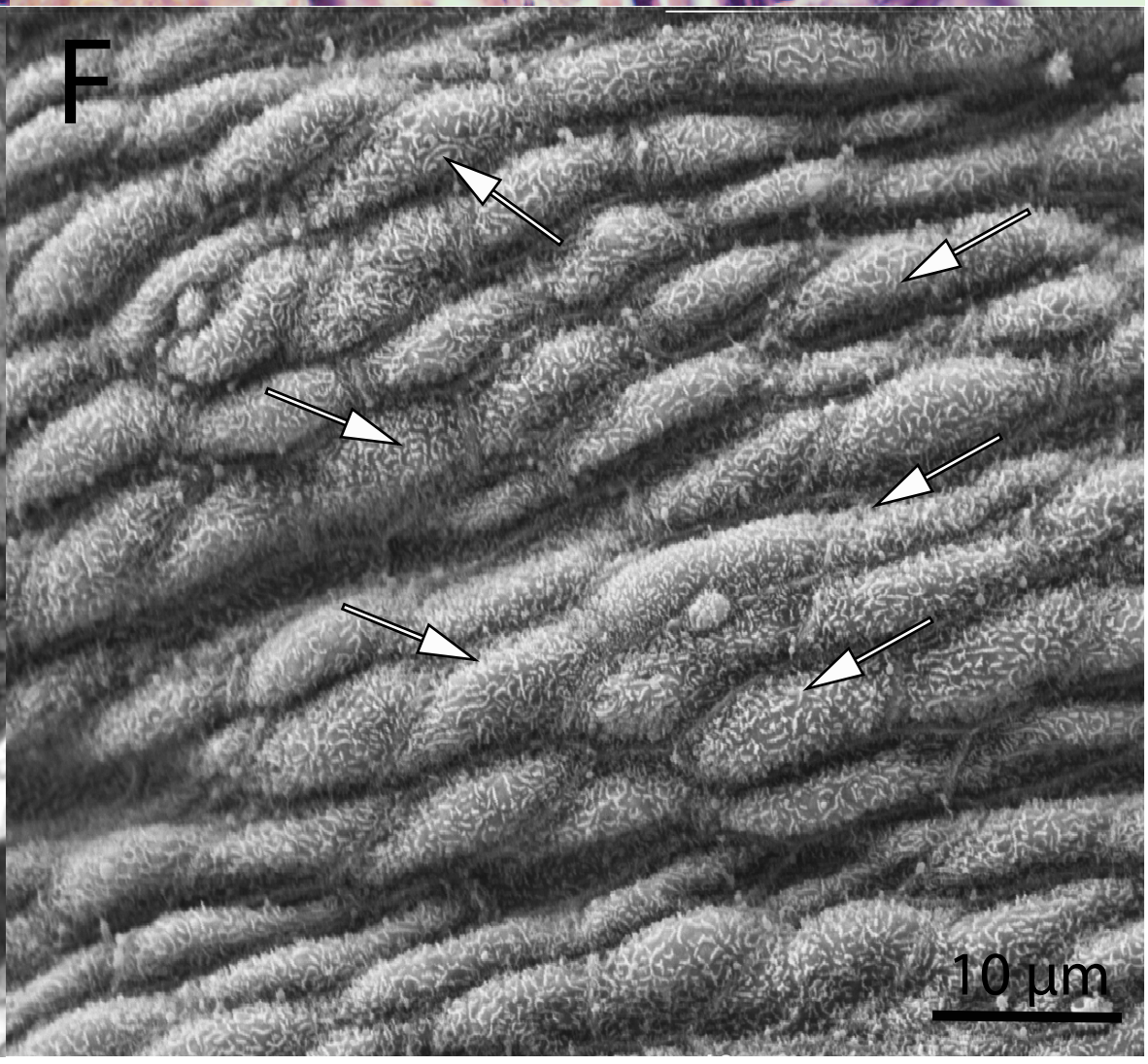

Figure 3

Click here to access/download;Figure;figure 3 non-implantation late pregnancy.pdf

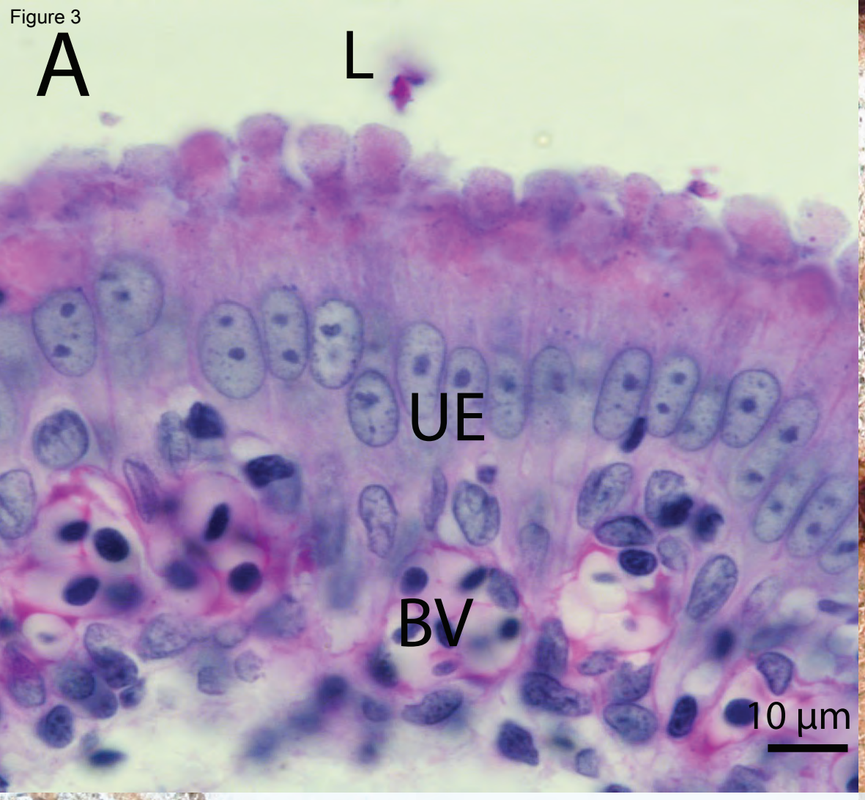

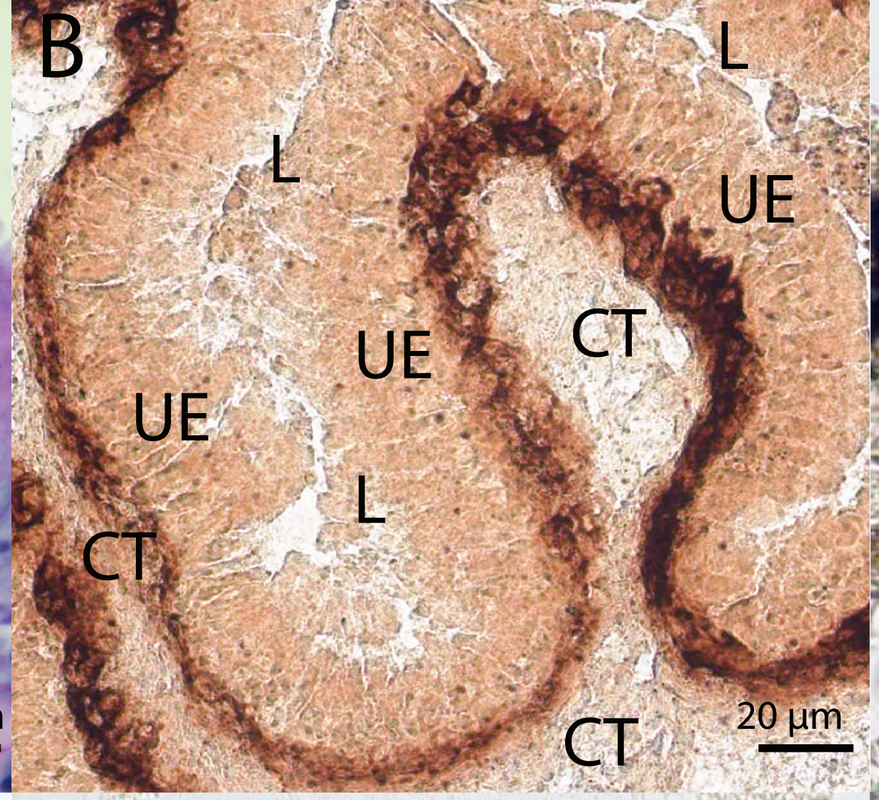

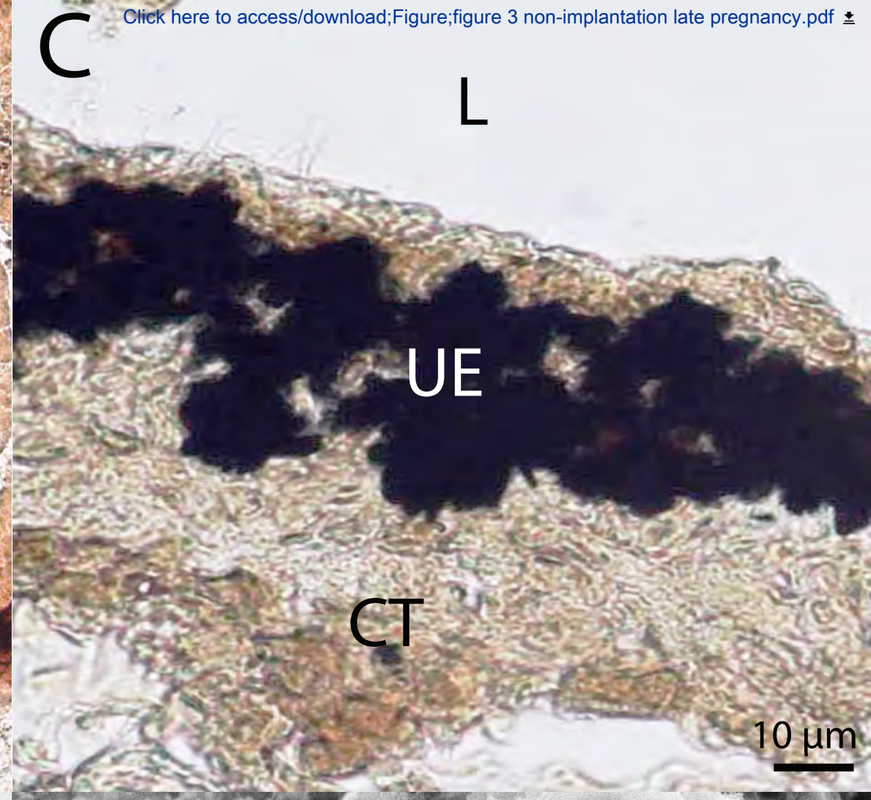

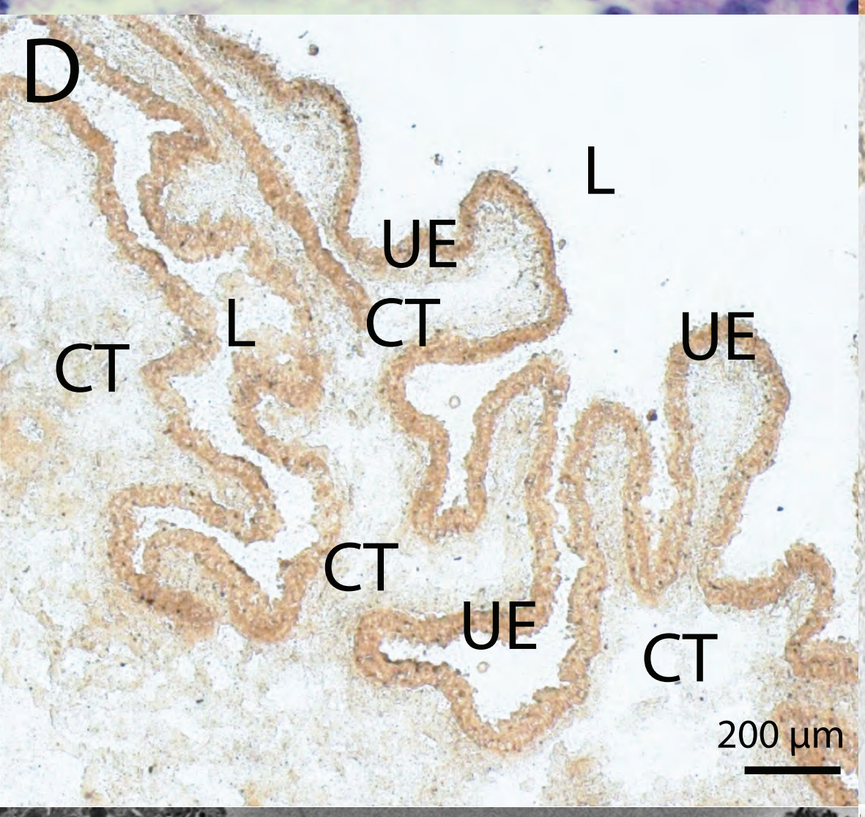

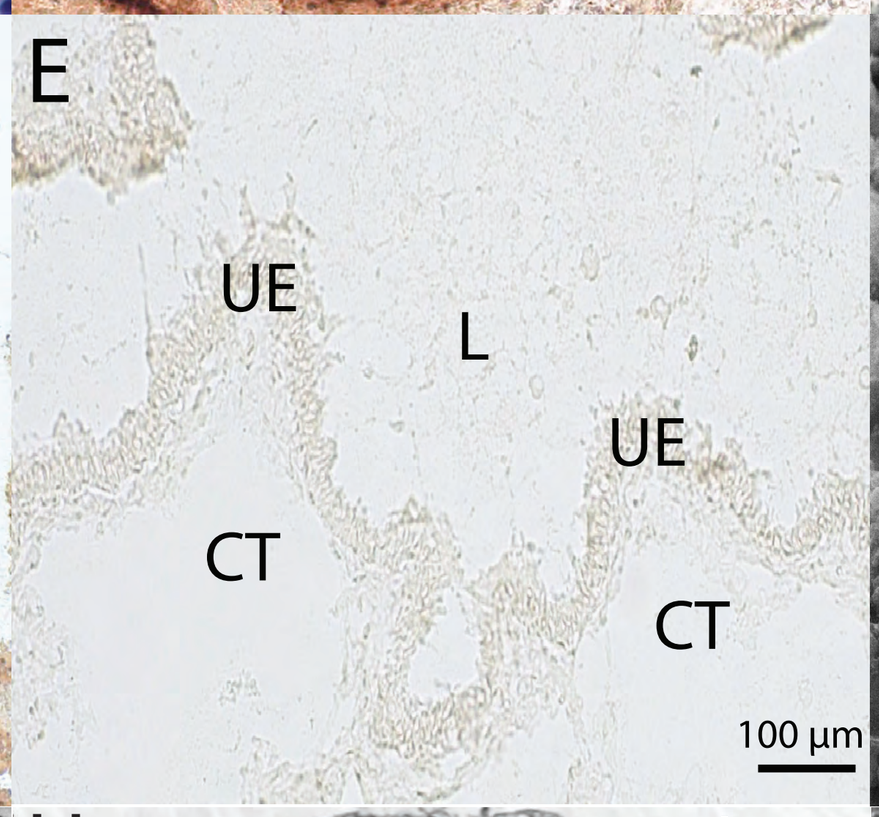

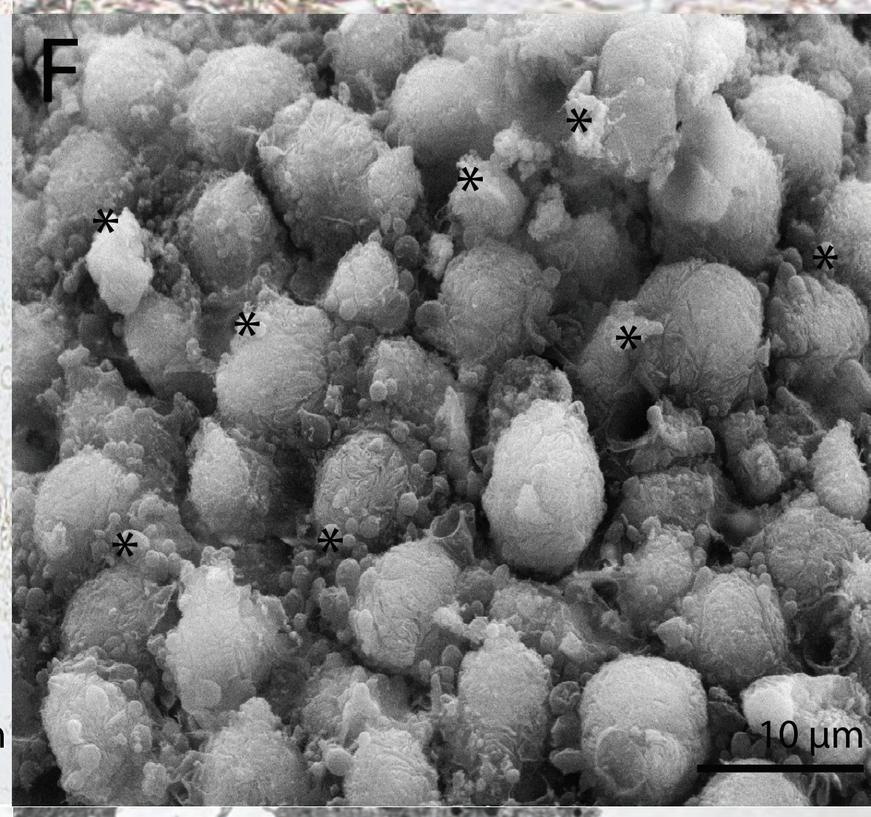

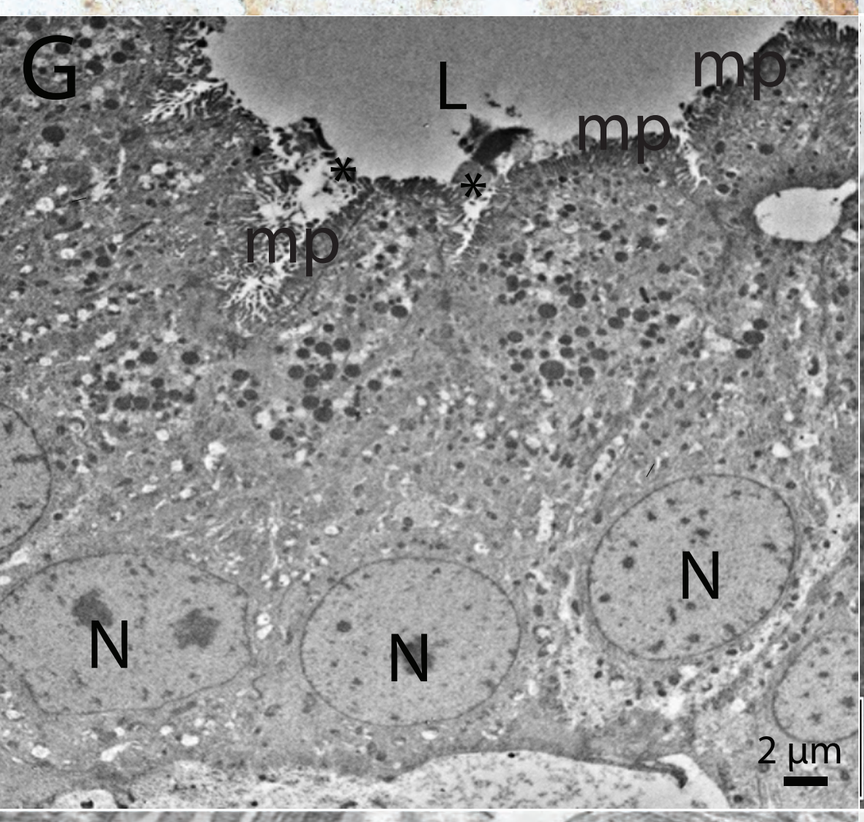

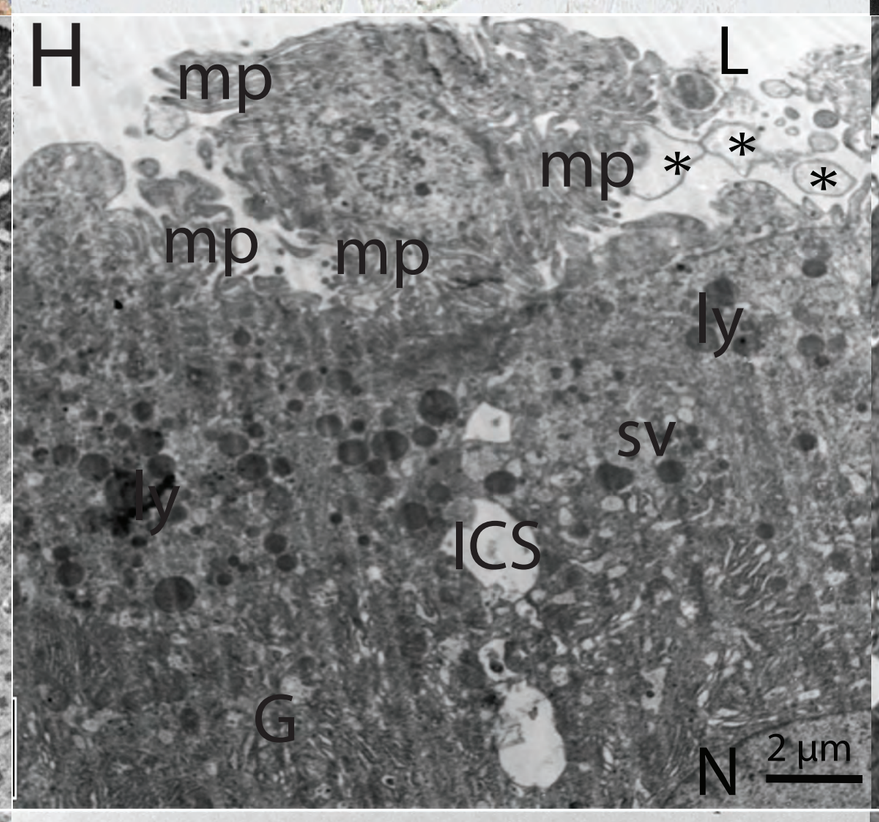

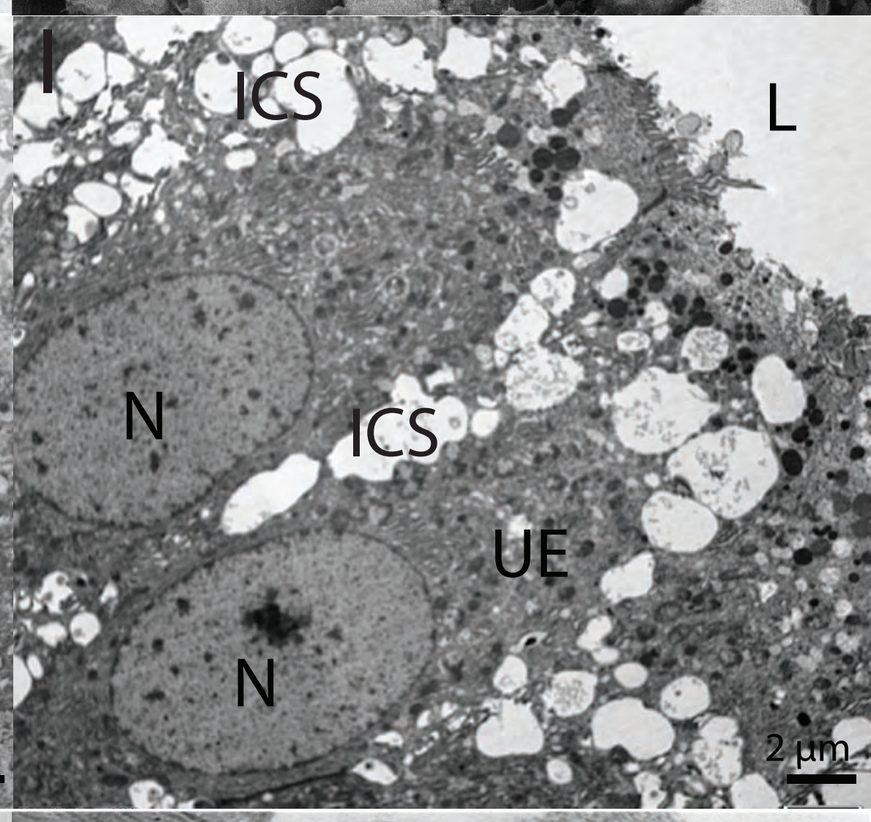

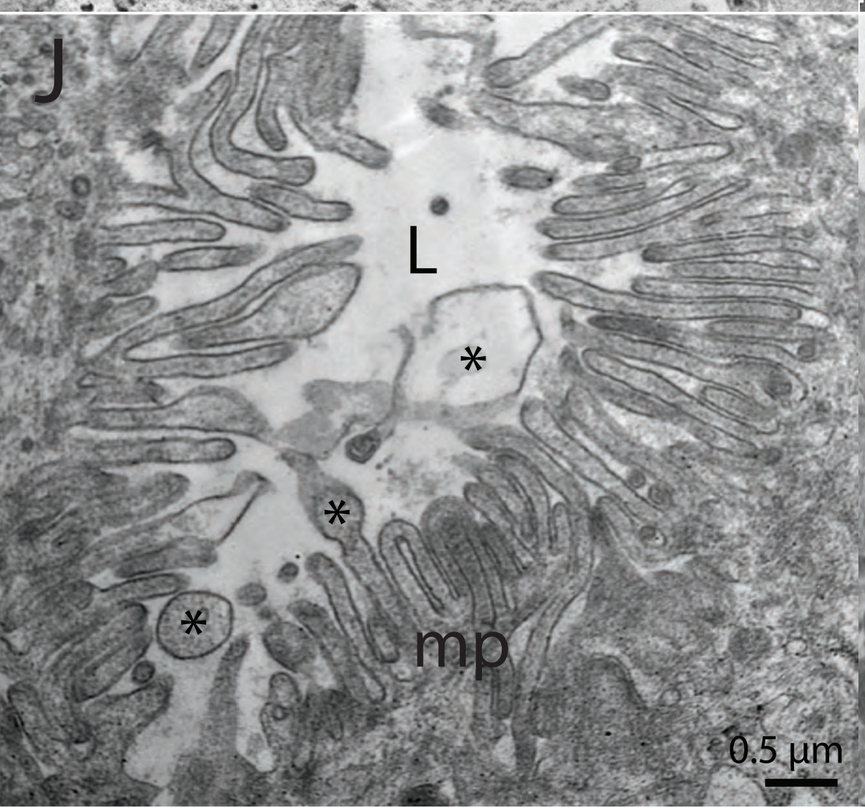

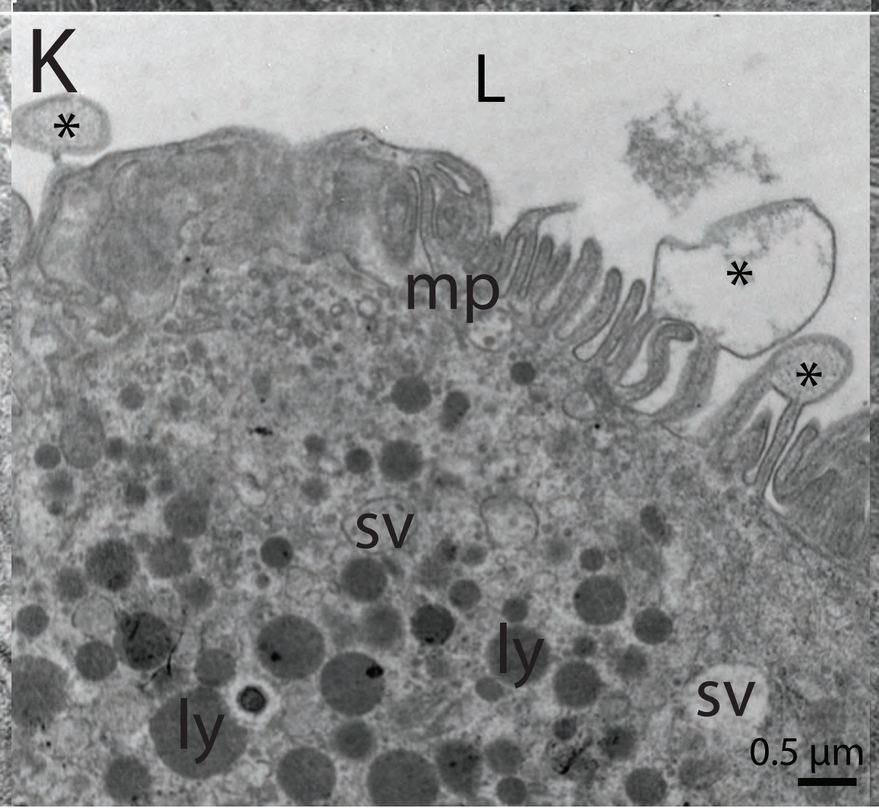

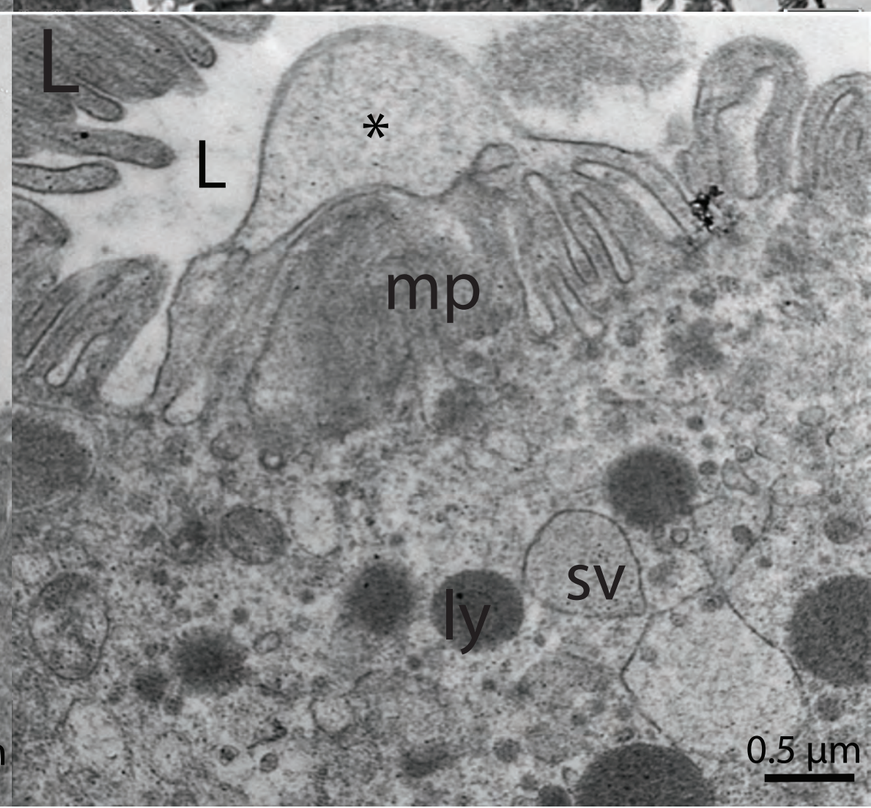

Figure 4

Click here to access/download;Figure;Figure 4. LM placenta + UC .pdf

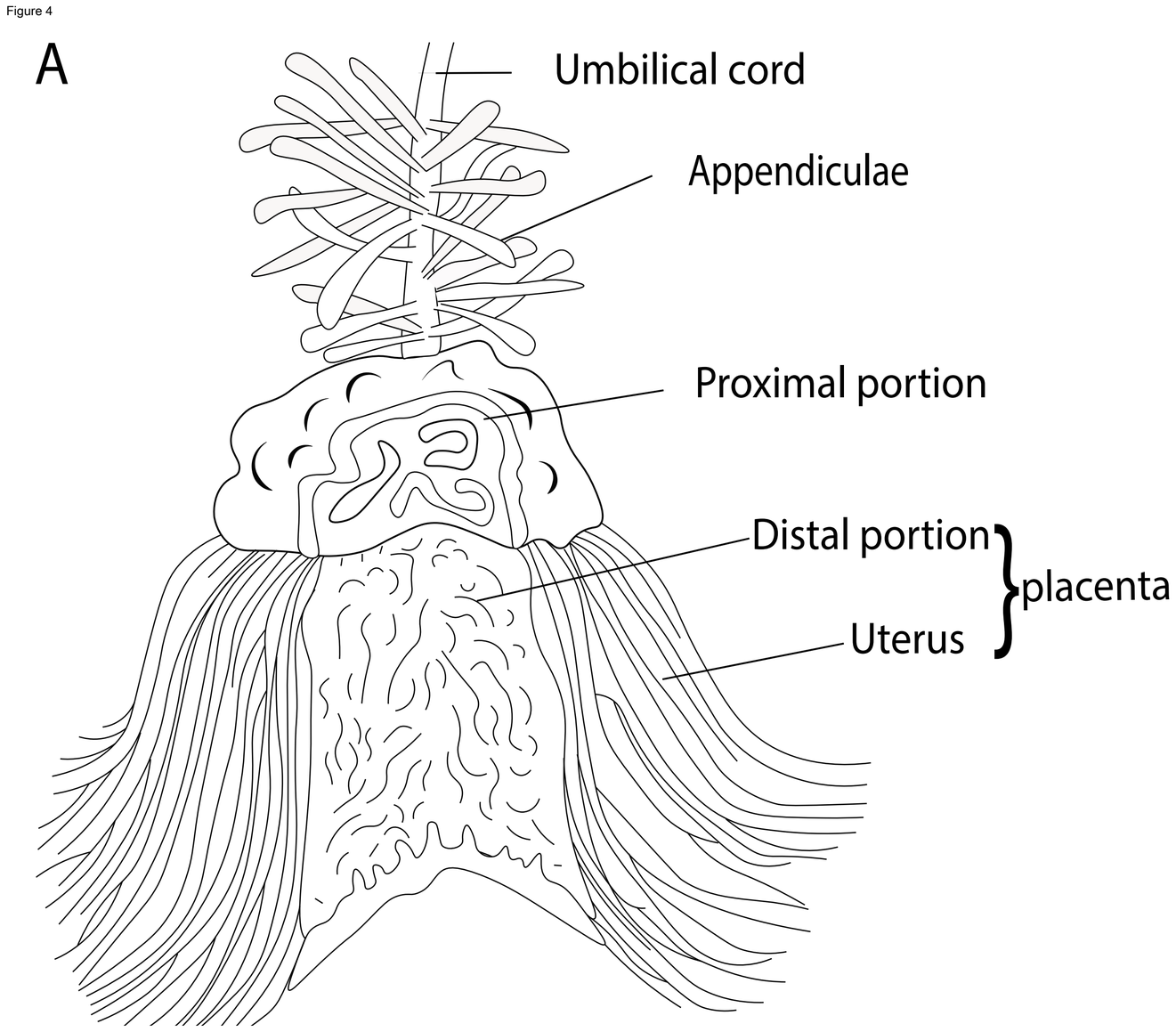

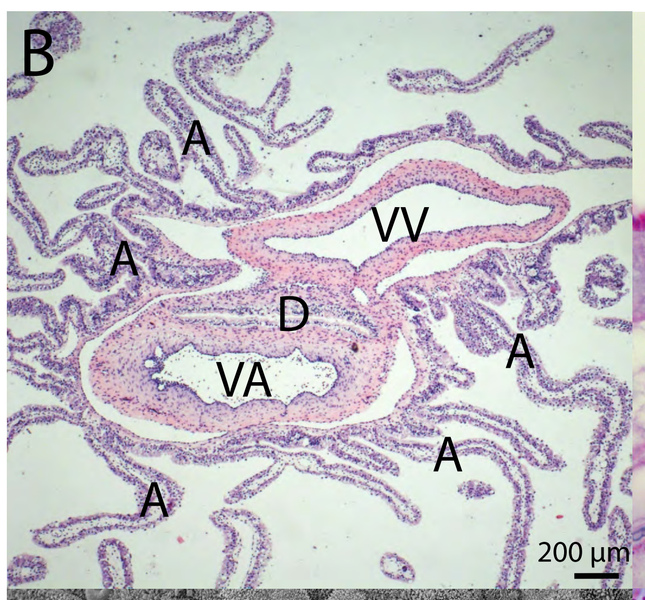

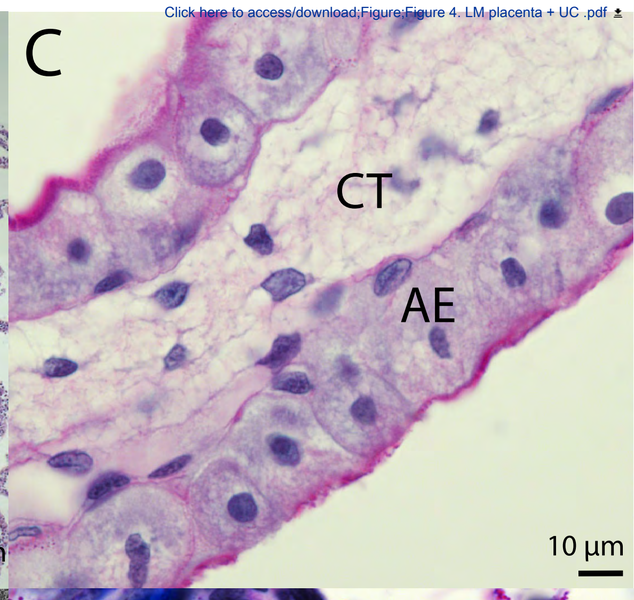

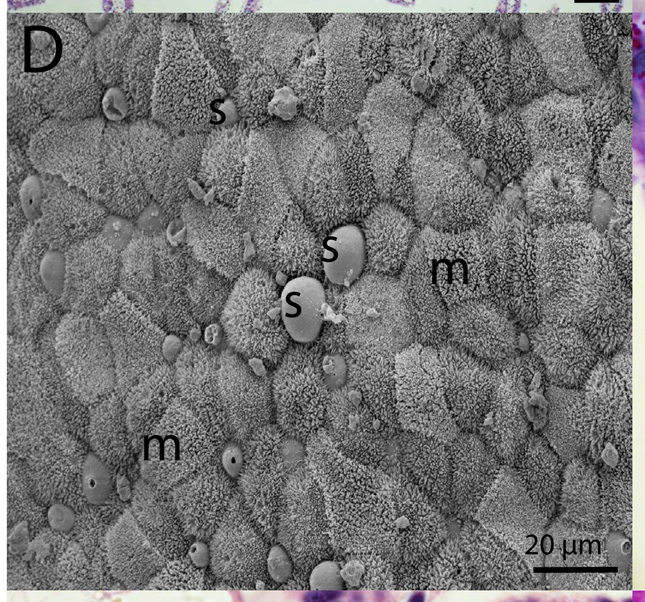

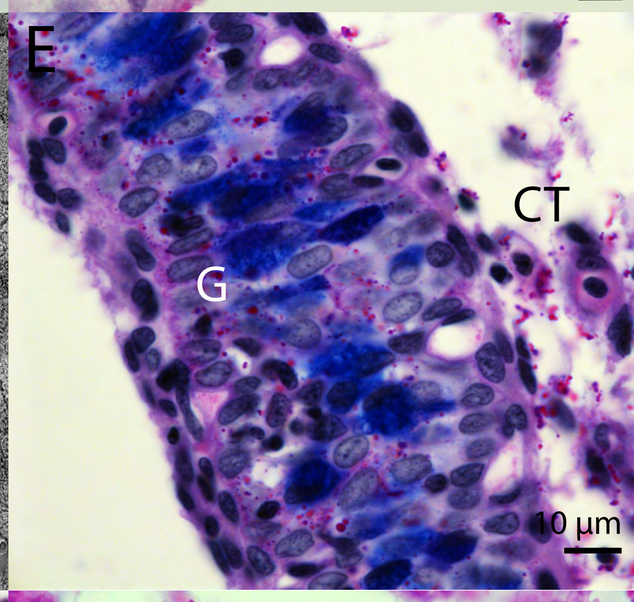

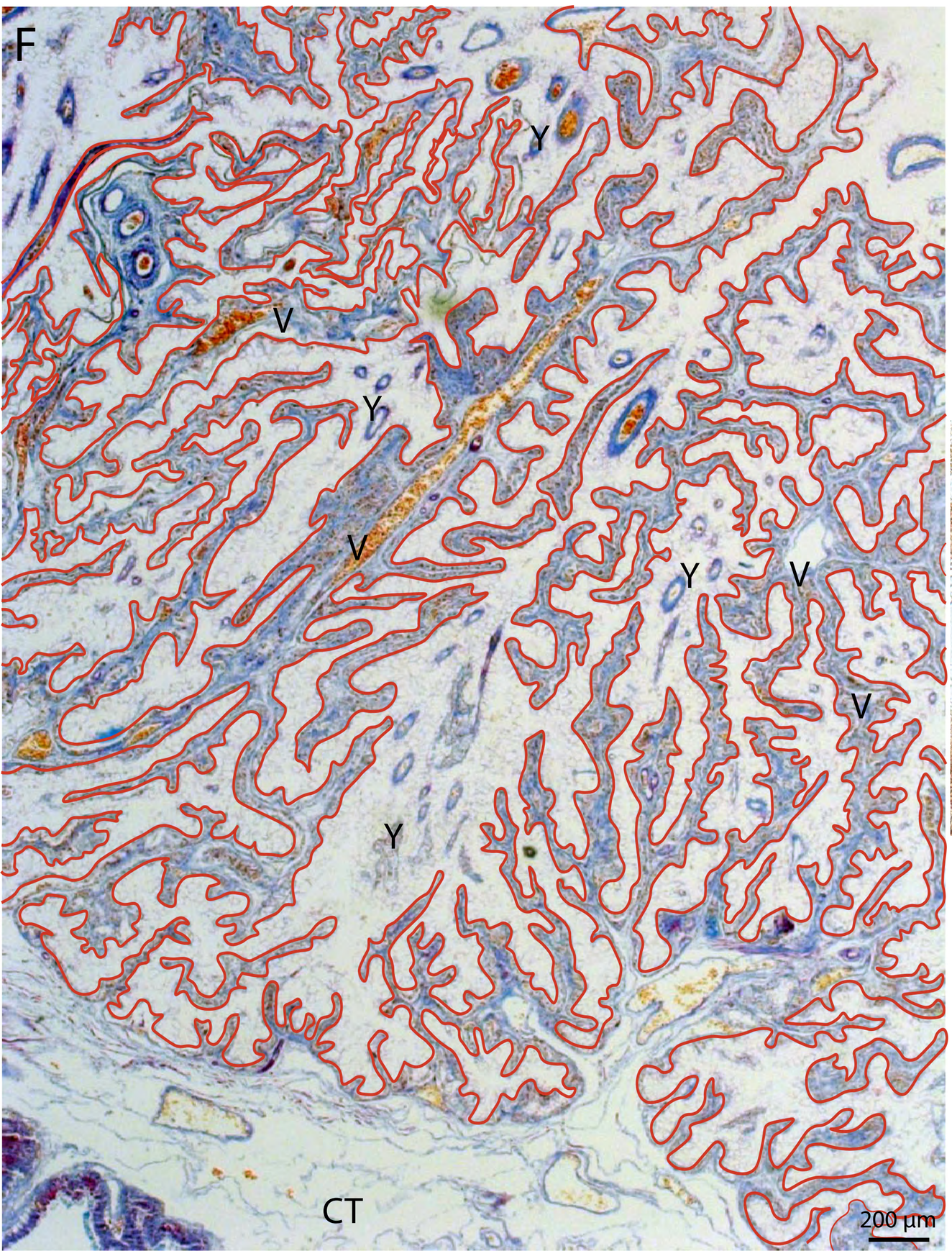

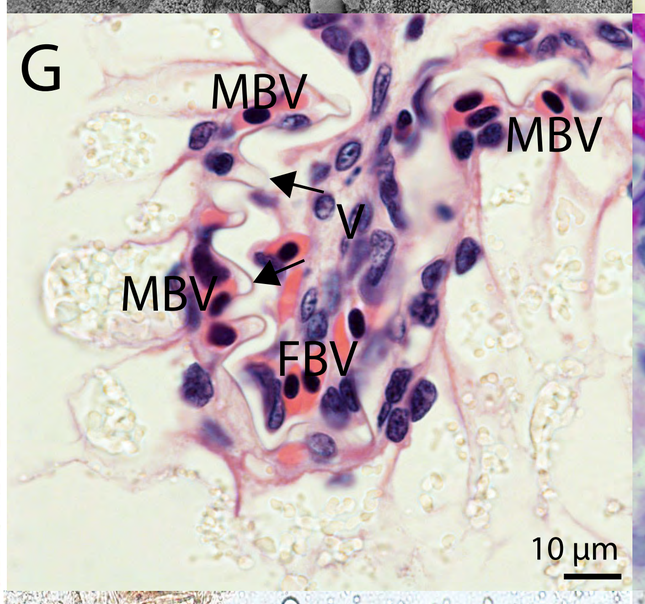

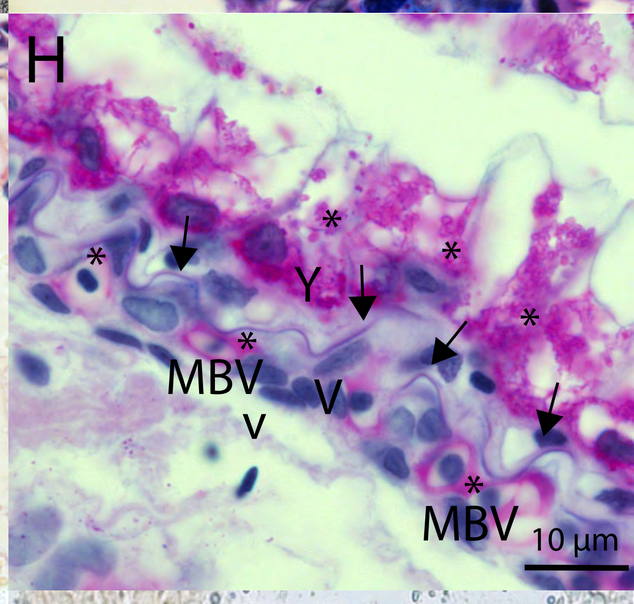

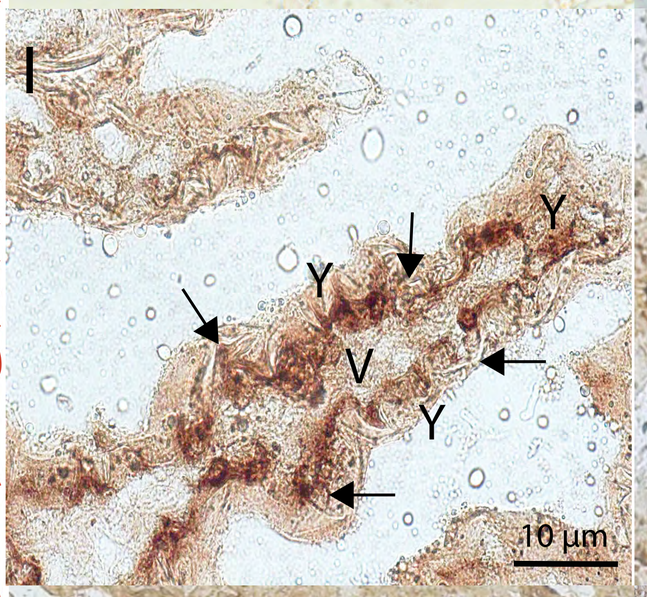

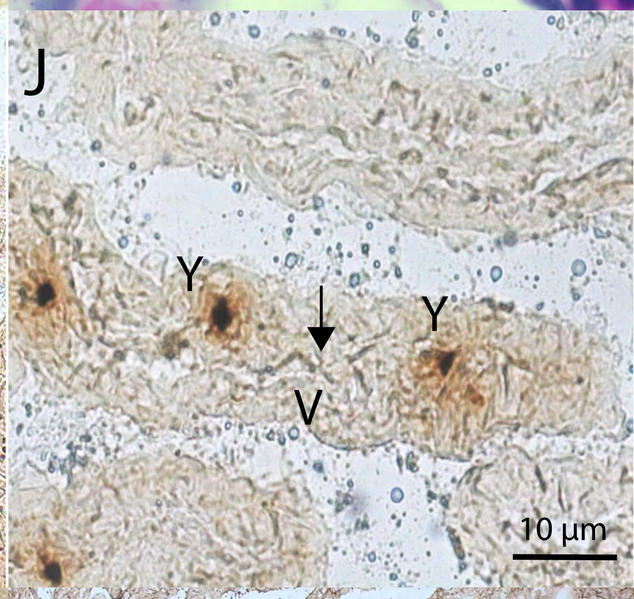

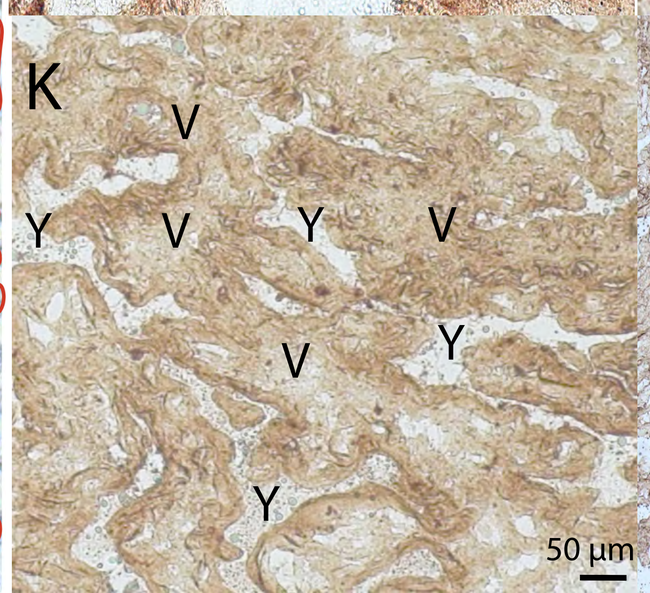

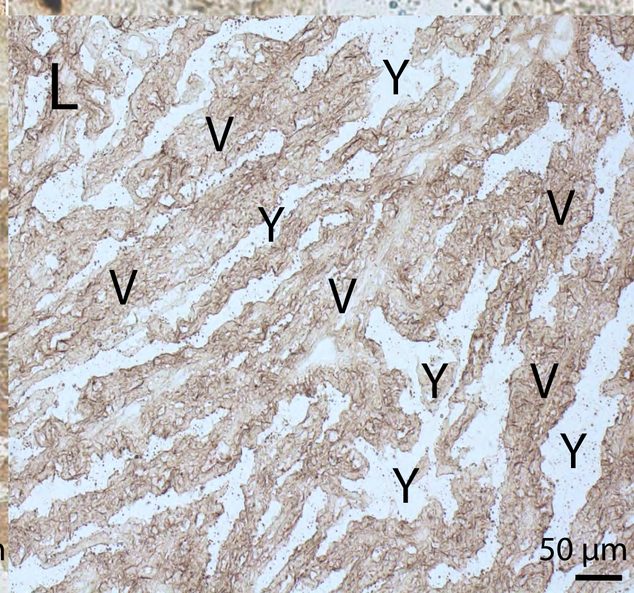

Figure 5

Click here to access/download:Figure;figure 5. TEM of the placental interface.pdf

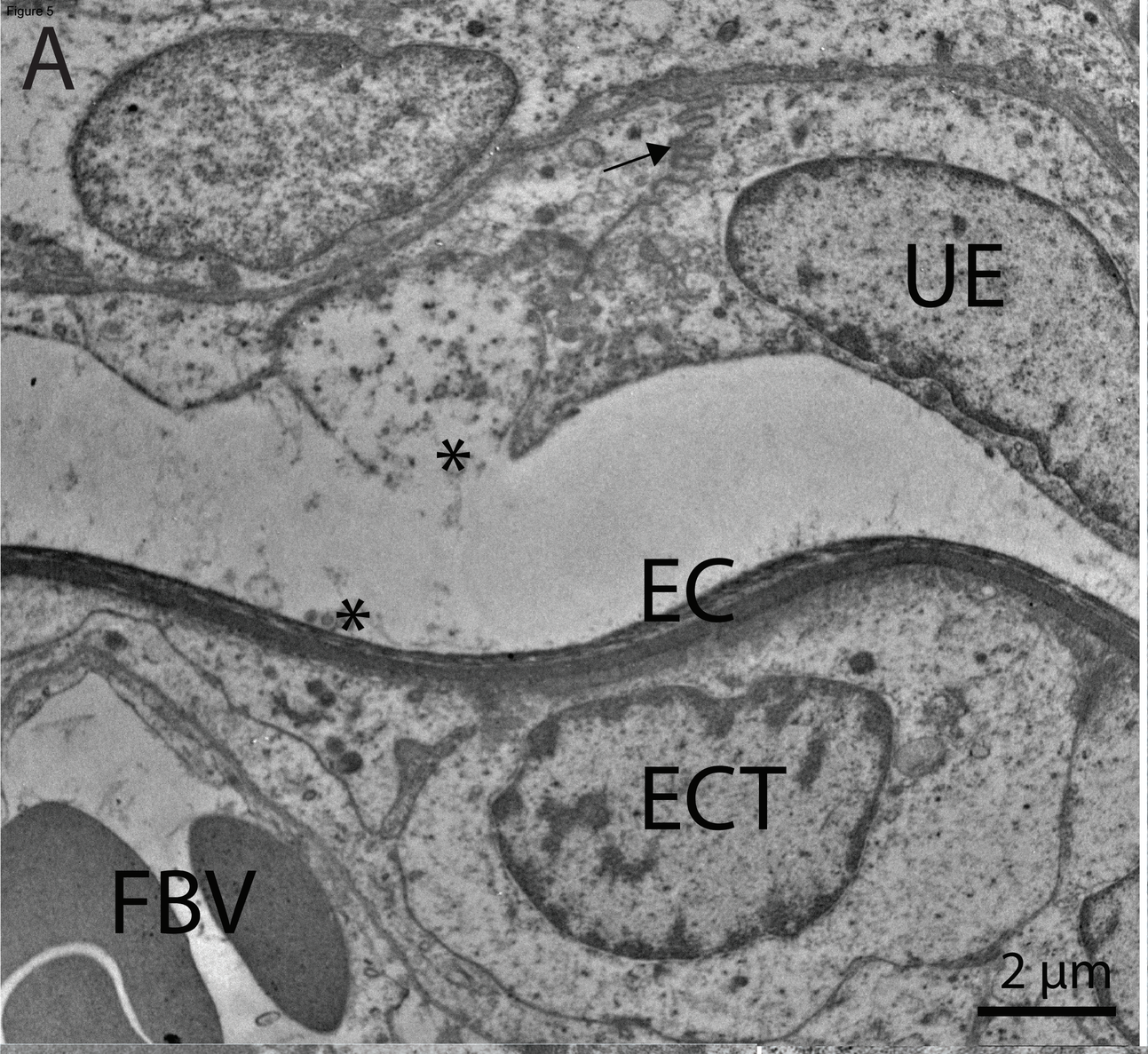

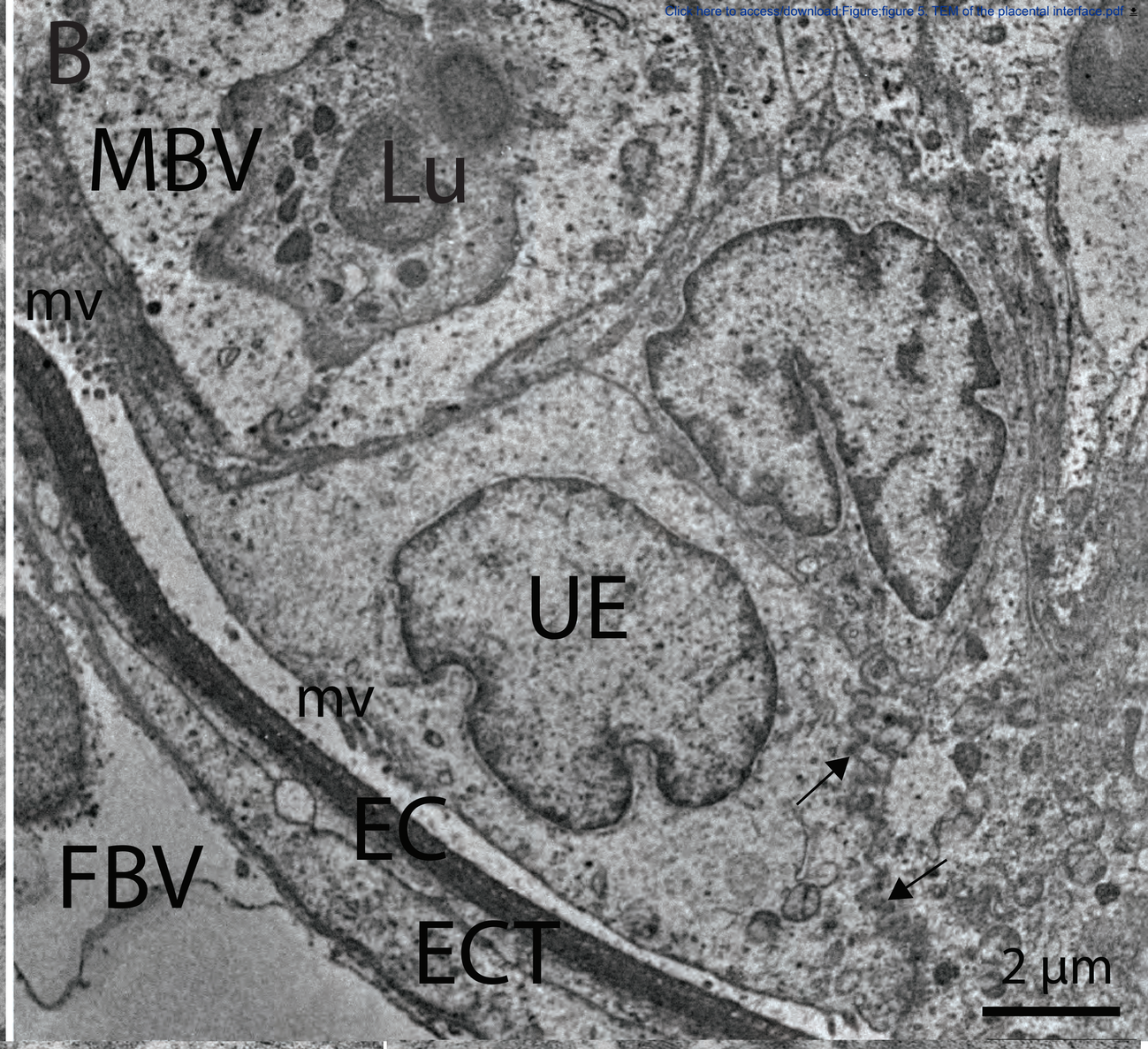

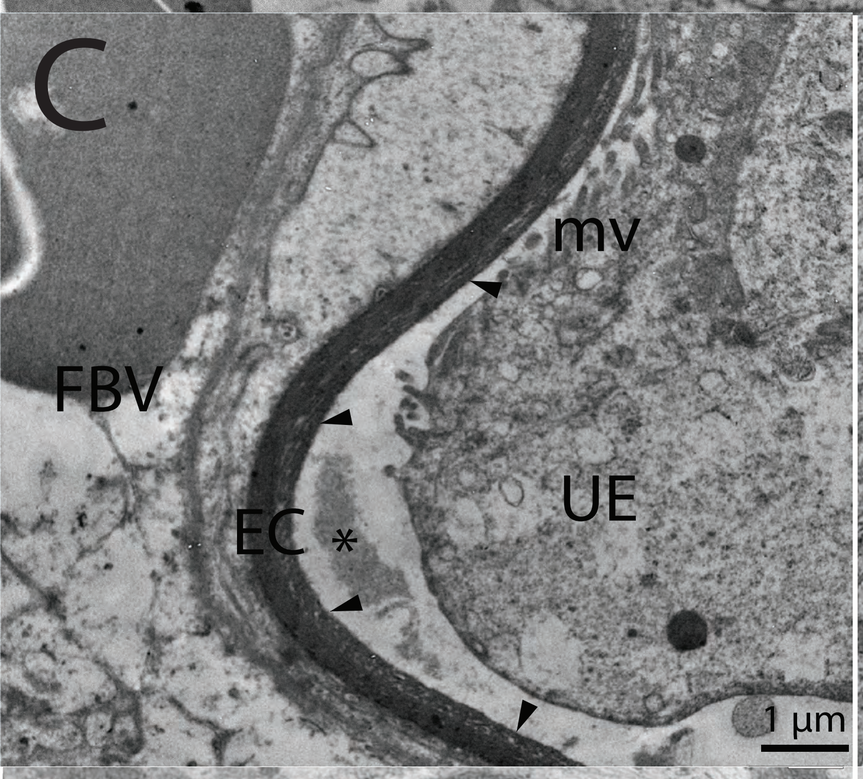

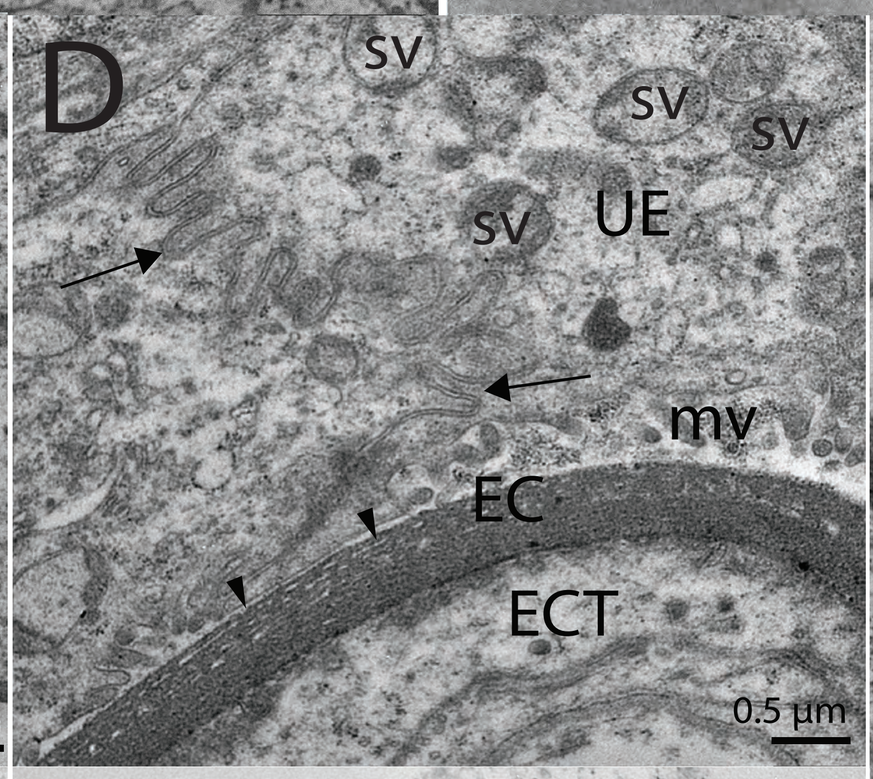

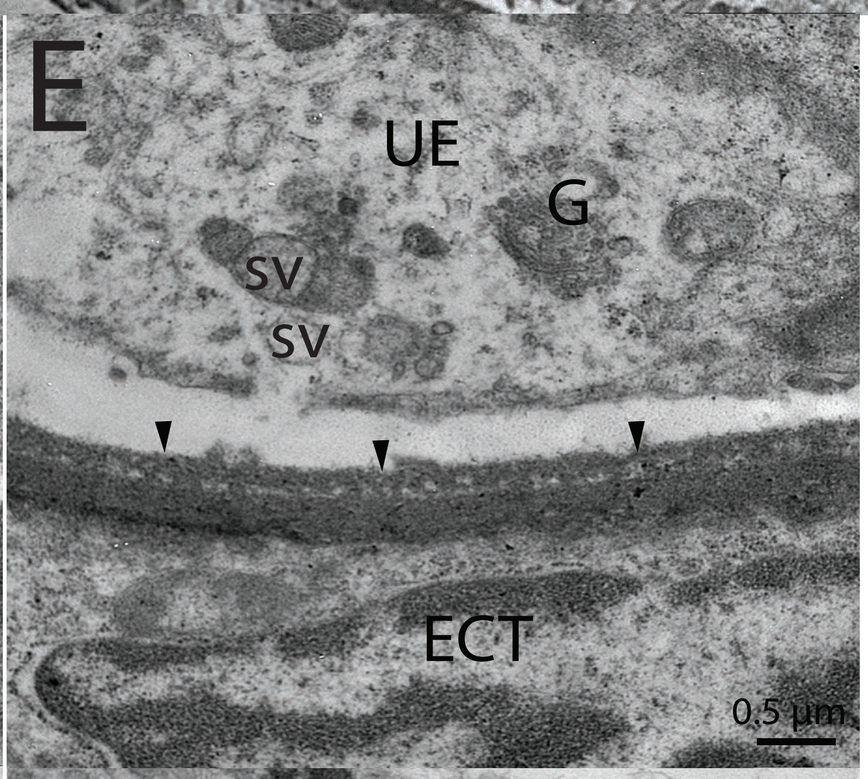

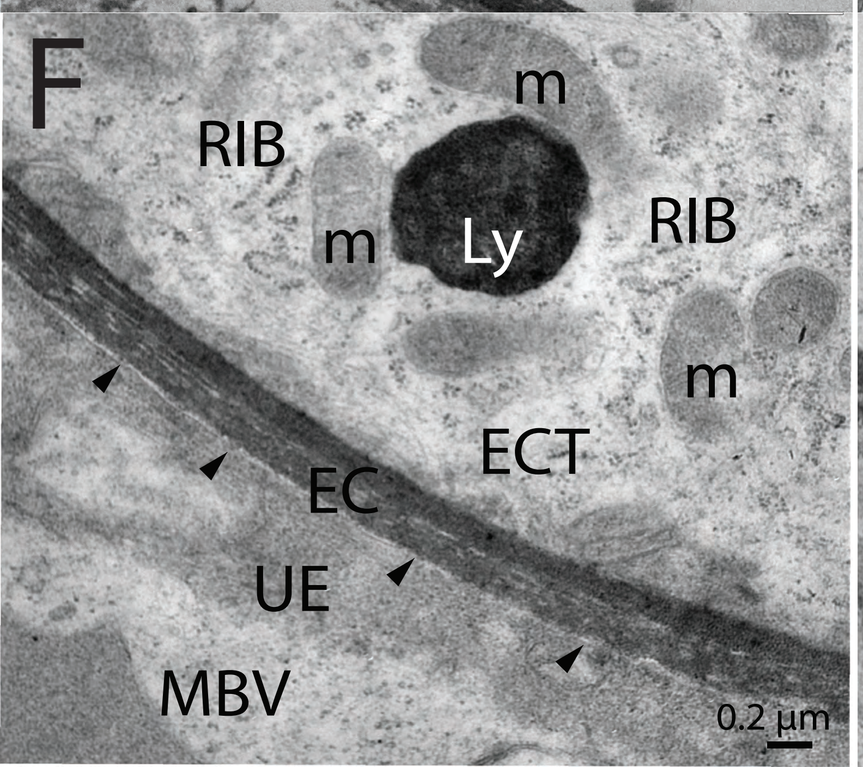

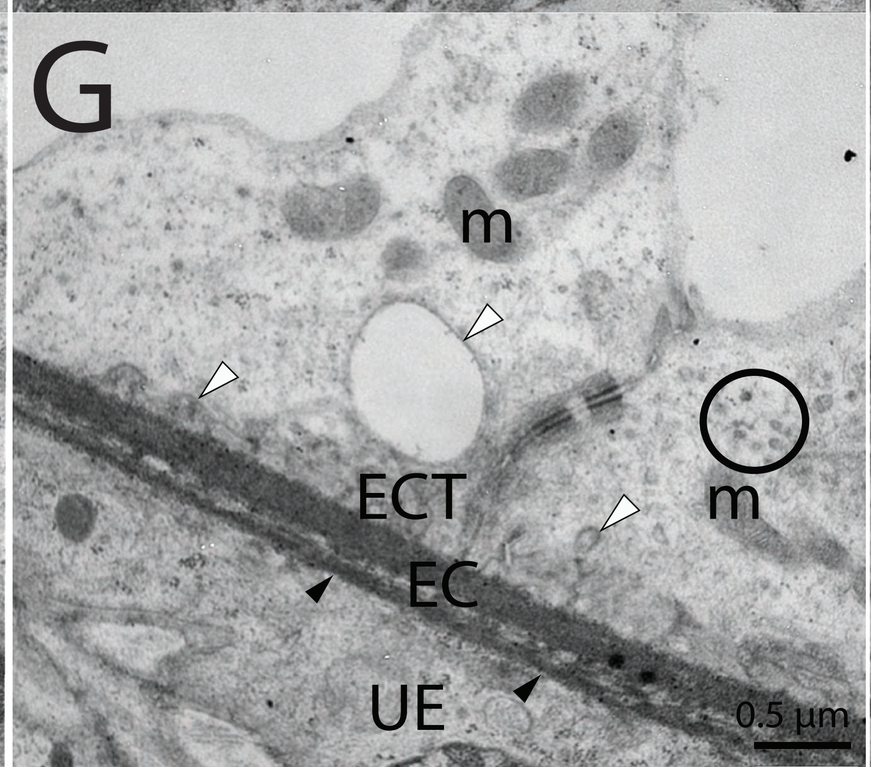

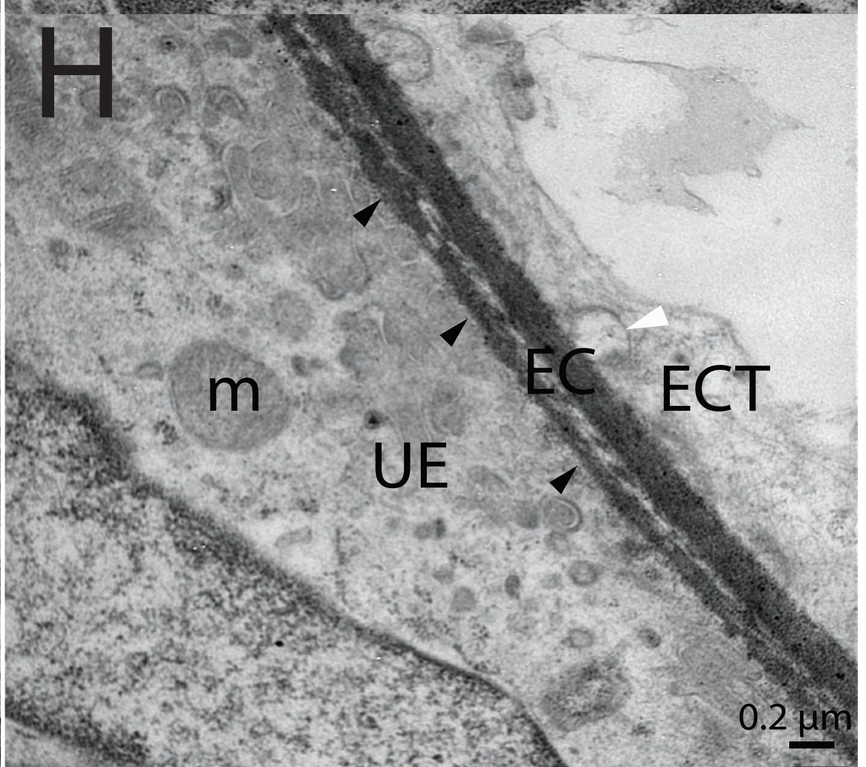

Figure 6

Click here to access/download;Figure;figure 6. caveolae .pdf

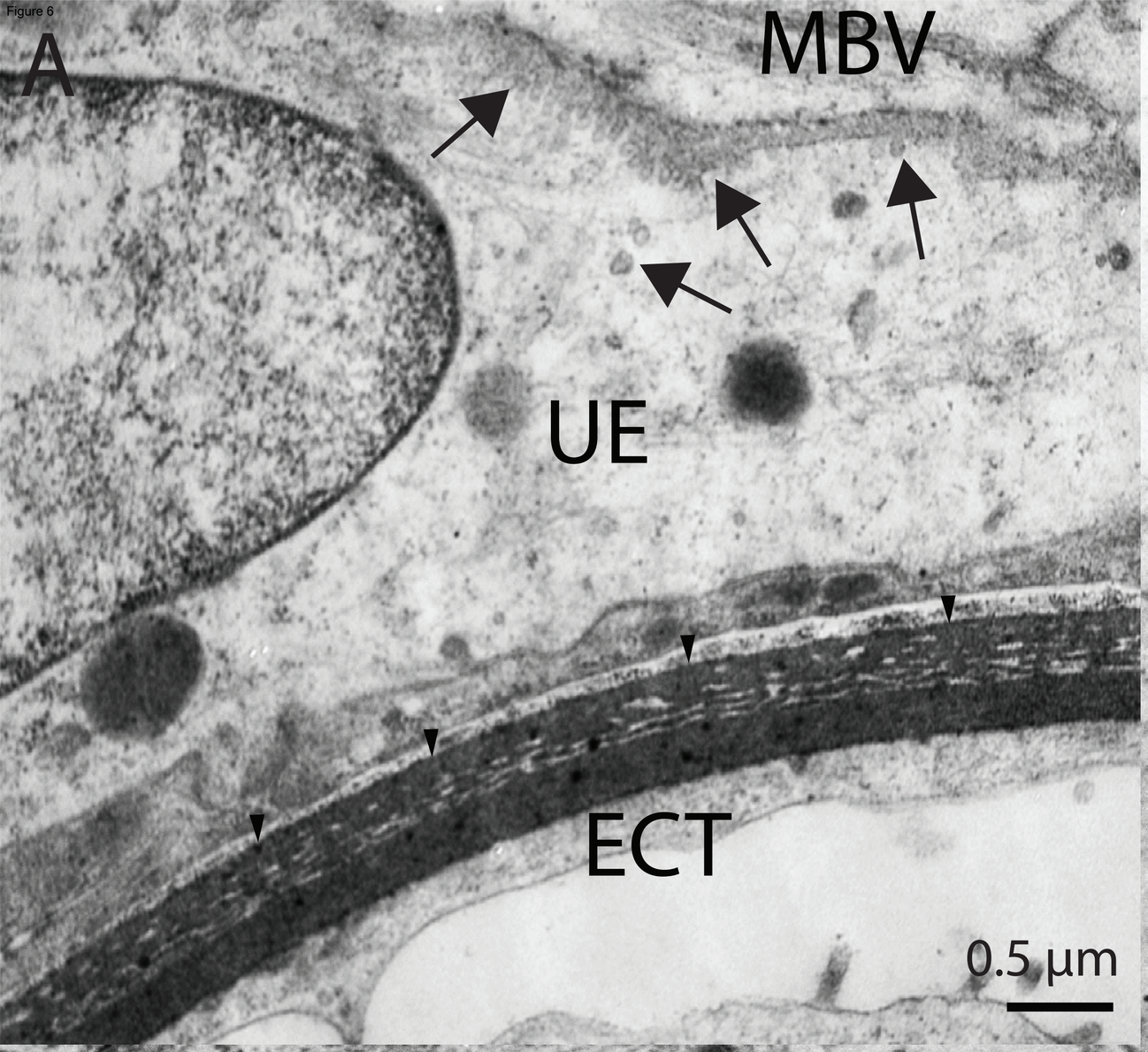

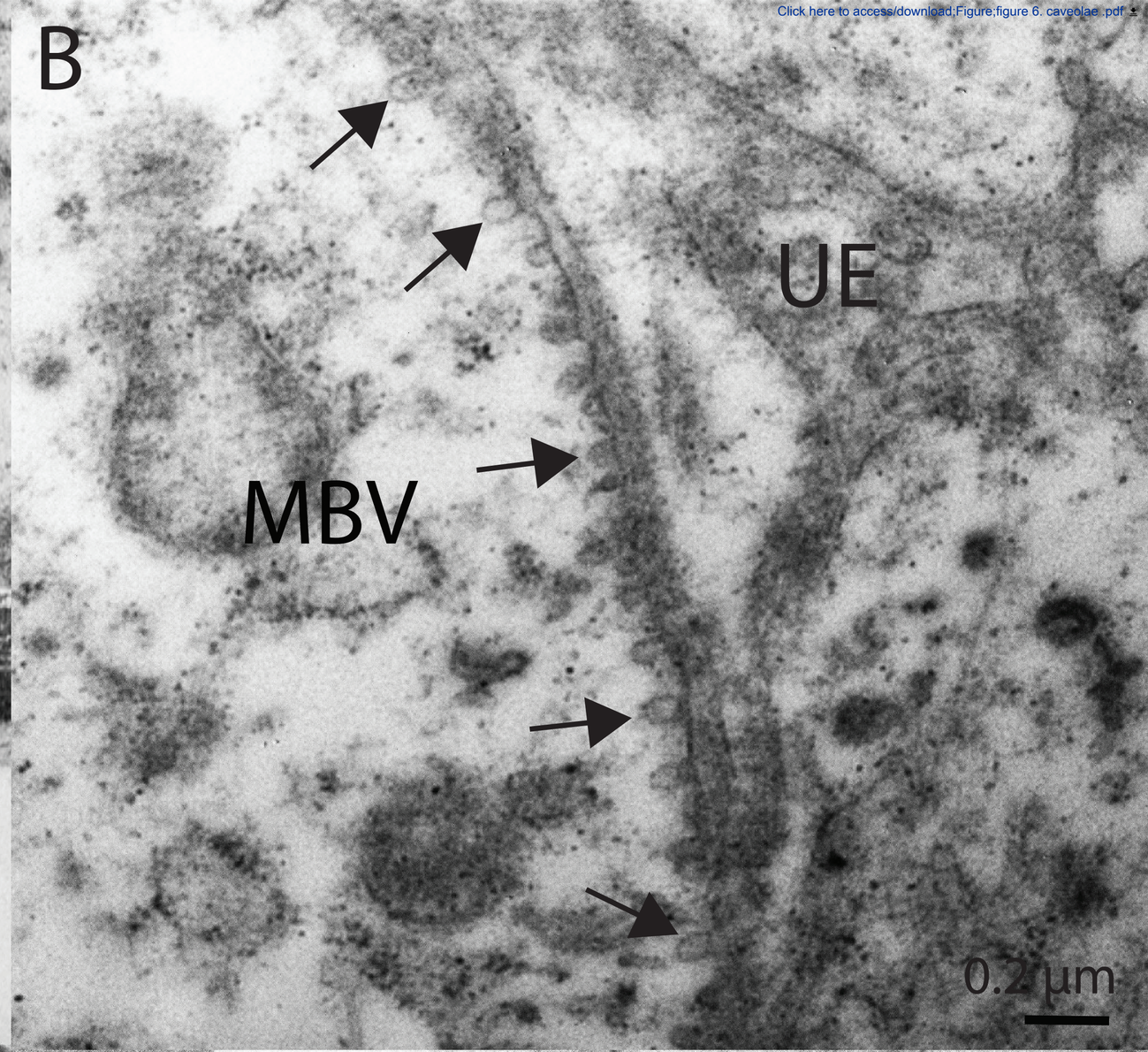

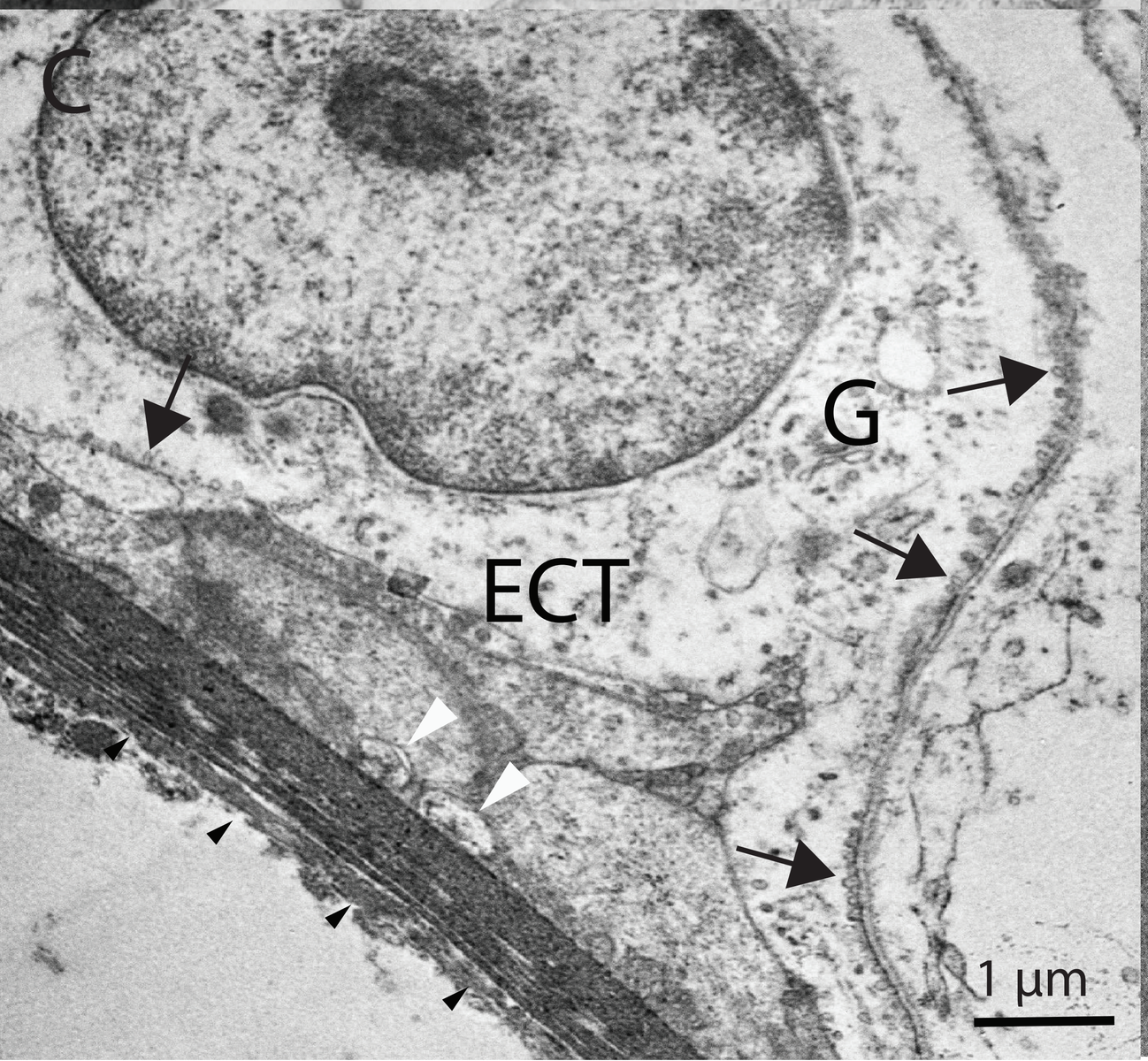

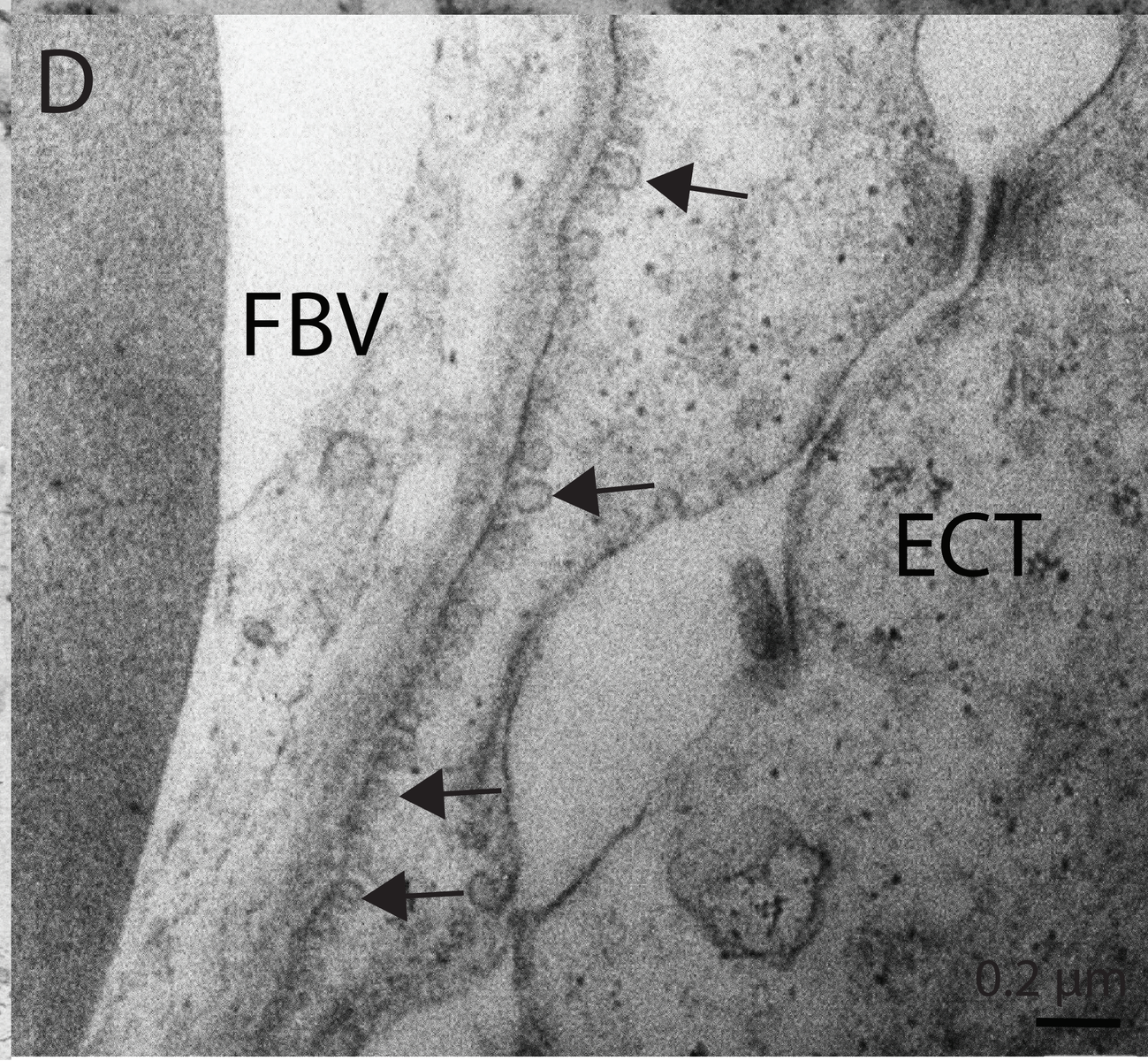

Figure 7

Click here to access/download;Figure;figure 7 BVs at interface.pdf